International Journal of Mass Spectrometry and Ion Processes 131 (1994) 355–385
0168-1176/94/$07.00

Sequencing of peptides in a time-of-flight mass spectrometer: evaluation of postsource decay following matrix-assisted laser desorption ionisation (MALDI)

R. Kaufmann*, D. Kirsch, B. Spengler

Institute of Laser Medicine, Heinrich-Heine-University, Moorenstrasse 5, D-4000 Duesseldorf, Germany

(Received 21 March 1993; accepted 2 July 1993)

Abstract

In matrix assisted laser desorption ionisation (MALDI) a large fraction of analyte ions undergo postsource decay (PSD) during flight in the field free drift path. By means of a modified two-stage reflectron, daughter ion time-of-flight spectra of medium sized linear peptides (up to 2800 u) were recorded containing full sequence information. Precision, accuracy and mass resolution of fragment ions were almost as good as obtained in high energy CAD studies performed in four-sector instruments. Instrumental sensitivity was better by at least one order of magnitude. In reflectron time-of-flight mass spectrometry (RETOF-MS) the cleavage pattern of PSD products is different from that obtained by high energy and low energy CAD. In our instrument, conditions which were energetically comparable to high energy and low energy CAD could easily and comparatively be studied in the same experiment by varying instrumental parameters. Activation mechanisms of PSD were found to be largely determined by collisional events (ion/neutral) induced by the acceleration field during early plume expansion. Future potentials of PSD analysis after MALDI are discussed.

Key words: Matrix-assisted laser desorption–ionization; Postsource decay; Collisionally-activated dissociation; Reflectron; Peptides

Introduction

Molecular structure elucidation by mass spectrometry has become a promising and rapidly expanding tool. The exploitation of collisionally-activated dissociation (CAD) of precursor molecules [1–3] has found its way into practical mass spectrometry and has considerably extended analytical applicability to molecular structure determination of e.g. oligopeptides. The most successful approach is based on tandem mass spectrometry, (MS-MS) with collisional activation (CAD) occurring in between a precursor-ion-selecting and a daughter-ion-analyzing mass spectrometer in sequence.

So-called high performance instruments, based on double focussing (four-sector) setups, allow efficient high energy activation and optimal mass resolution for both precursor selection and fragment analysis, but, due to their high cost, they are difficult to afford for routine analysis. More popular approaches use quadrupole filters either as triple-quad arrangements or as hybrids. The latter employ a double focussing mass spectrometer for improved precursur ion selection. Both hybrids as well as triple-quads share the problem of accepting precursor ions at rather low kinetic energies only (E_{lab} = 10–50 eV).

Several comparative studies [4–6] indicate that for peptide sequencing low energy CAD is restricted to precursor ion masses below about

* Corresponding author.

SSDI 0168-1176(93)03876-N

800 u and, thus, is of limited usefulness. Some improvement was recently attained by increasing the kinetic ion energy in such hybrids to 500 eV (E_{lab}) [7]. There is, however, a rather general consensus that, even under the conditions of high energy CAD (up to 10 keV E_{lab}), which is typical for four-sector tandem instruments, fragmentation efficiency rapidly degrades with precursor masses above 2000 u. Some recent attempts to circumvent the efficiency problem by employing surface induced dissociation (SID) instead of CAD [8,9] have not yet found broad application.

It appears then, that all practical means to considerably improve efficiency of collisionally activated dissociations in larger peptides by dumping more collisional energy into the analyte molecule have been exhausted.

There is, however, a second but widely neglected parameter in CAD (and possibly SID) experiments, namely time. Dissociations induced by collisional energy transfer are anything but prompt events, especially in large polyatomic ions. Calculations of metastable decay rates in model oligo/polypeptides [10–12] based on the RRKM theory

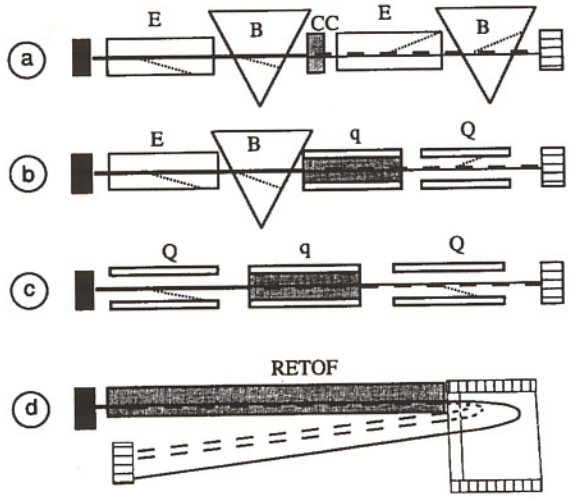

Fig. 1. Comparative schemes of setups for mass spectrometric analysis of collisionally activated product ions. (a), Four-sector instrument (EBEB); (b), hybrid instrument (EBqQ); (c), triple Quad; (d), RETOF-mass spectrometry (——), stable precursor ions: (- - -), transmitted ions: (· · ·), non-transmitted daughter ions. Areas indicating possible sites of fragmentation are shaded.

or derivatives thereof indicate that, for ions larger than say 1500 u, the chance to decompose within typical mass spectrometric time scales (10^{-5} to 10^{-4} s) steeply diminishes.

From this point of view four-sector instruments are rather unfavourable devices. On the one hand, precursor ions must survive the long passage through MS 1 ($\approx 50\,\mu$s), thus only "cool" species will reach the collision chamber. On the other hand, once they have collided they are expected to decay almost immediately, i.e. in a short time interval of e.g. 1 μs before they enter MS 2 (see Fig. 1). Hence, with increasing precursor masses (and thus lower decay rate) this type of instrument must run into conflicts even at the highest possible levels of collisional activation (see also ref. 13).

Hybrids or triple quads, however, provide for a much longer time window (40–100 μs) but suffer from an inherently low level of collisional excitation unless, perhaps, ions are multiply charged as in electrospray ionisation (ESI) and/or are pre-excited [14–17].

In this situation we propose to evaluate time-of-flight (TOF) mass spectrometry as a possible alternative to, or, for some applications, even as a substitute for conventional MS-MS. Although this suggestion might appear rather ambiguous at first glance, we will demonstrate, by means of only a few minor modifications, that a simple reflectron TOF mass spectrometer (RETOF-MS) can be operated so as to reach performances in product ion analysis comparable to those of the most advanced tandem instruments.

Metastable ion analysis is a well known technique in RETOF mass spectrometry [18–22]. The first successful attempts to sequence peptides by metastable-ion analysis have been demonstrated by Tang et al. [19,20] employing particle induced desorption for precursor ion formation. With the advent of matrix-assisted laser desorption (MALDI), extremely efficient pulsed ion sources for larger peptides and proteins emerged [23, 24] and are about to become (along with ESI) the standard approach to practical mass spectrometry for larger peptides and proteins.

Recent investigations in our laboratory [25,26] have demonstrated that in MALDI a large fraction of the desorbed analyte ions undergo fragmentation-neutralisation reactions during flight. The activation energy for this kind of "postsource-decay" (PSD) apparently stems from: (1) multiple early collisions between analyte ions and (neutral) matrix molecules during plume expansion and ion acceleration; (2) from collisional events with residual or admitted gas molecules in the field free drift path. Thus, MALDI-RETOF mass spectrometry is rather unique in providing for: (1) highly pre-excited precursor ions which (2) move at high kinetic energy over a relatively long distance (time window) where they can undergo (3) either unimolecular decomposition and/or (4) can be further activated by collisions with residual or other gas molecules (see Fig. 1). The main characteristics of the different instruments used for CAD product ion mass spectrometry are listed in Table 1 for comparison.

In a recent report [26] we have already demonstrated that a RETOF setup can be exploited to obtain full sequence information from PSD fragment ions of medium sized peptide precursors (1600 u) produced by MALDI. In the present paper we explore this approach more extensively with respect to the requirements of practical mass spectrometry and to its possible merits vis-a-vis conventional MS-MS.

Experimental

General description of the setup and sample preparation

The RETOF-MS used was basically a modified LAMMA 1000 type setup (Fig. 2). For laser

Table 1
Main characteristics of instrumentation used for CAD product ion mass spectrometric analysis

	Four-sector tandem MS	Hybrids (BEqQ)	Triple Quad	RETOF (PSD-MALDI)
Ion source	FAB/CF-FAB	FAB/CF-FAB	FAB, ESI	MALDI
Collisional activation	High energy (up to 10 keV E_{lab})	Low energy (20–50 eV)	Low energy with pre-excitation (ESI)	High energy (in flight), adjustable high pre-excitat. (in source), adjustable
Time window available for ion decay	Short (2–5 μs)	Long (20–30 μs)	Long (20–30 μs)	Very long (30–300 μs) adjustable in limits
Transmission of precursor ions	15%	6–8% (Mismatch of energy acceptance)	2%	≈ 50%
Transmission of products (fraction of total product ions formed)	0.03% 3% with array detector	0.1%	0.1%	> 50% 8–10% at acceptable mass resolution
Interference with matrix product ions	Yes	Yes	Yes	No (no isobaric ions formed)
Precursor ion selection	High resolution required and possible	High resolution required and possible	High resolution required, not possible	High resolution not required, low resolution possible

desorption, pulsed laser light of either a N_2 laser ($\lambda = 337$ nm) or a fourth-harmonic Nd-YAG laser ($\lambda = 266$ nm) could be transmitted and focussed onto the sample by means of 90° incident focussing optics, described below. Vacuum conditions were typically $(5–6)\times10^{-7}$ Torr through a $16\,m^3\,h^{-1}$ rotary pump followed by two turbomolecular pumps ($150\,l\,min^{-1}$ and $330\,l\,min^{-1}$ respectively). Samples were prepared in the usual way by blow drying about 1–10 μl of sample solution ($\approx 10^{-2}$ M dihydrobenzoic acid (DHB) and $\approx 10^{-5}$ M analyte in aqueous solution) on a polished aluminium substrate. The sample could be imaged through the focussing optics by means of a CCD camera; the *x-y-z* position was controlled manually by micrometer translation stages.

Ion formation and extraction, and precursor selection

Laser focussing, sample imaging and ion acceleration-extraction were all performed coaxially and perpendicularly to the sample surface by means of a combined optical-ion-optical device. The optical part consists of a quartz triplet lens (numerical aperture ≈ 0.3) bearing a central bore (6 mm diameter) for ion transmission. Ion acceleration and collimation is performed by an assembly of diaphragms located within the free working distance (≈ 32 mm) between the front lens and the sample plane. The first part of the field free drift path is formed by a rather narrow tube (diameter 6 mm, length 180 mm), tapering the central bore of the triplet lens assembly. At the exit of this tube a

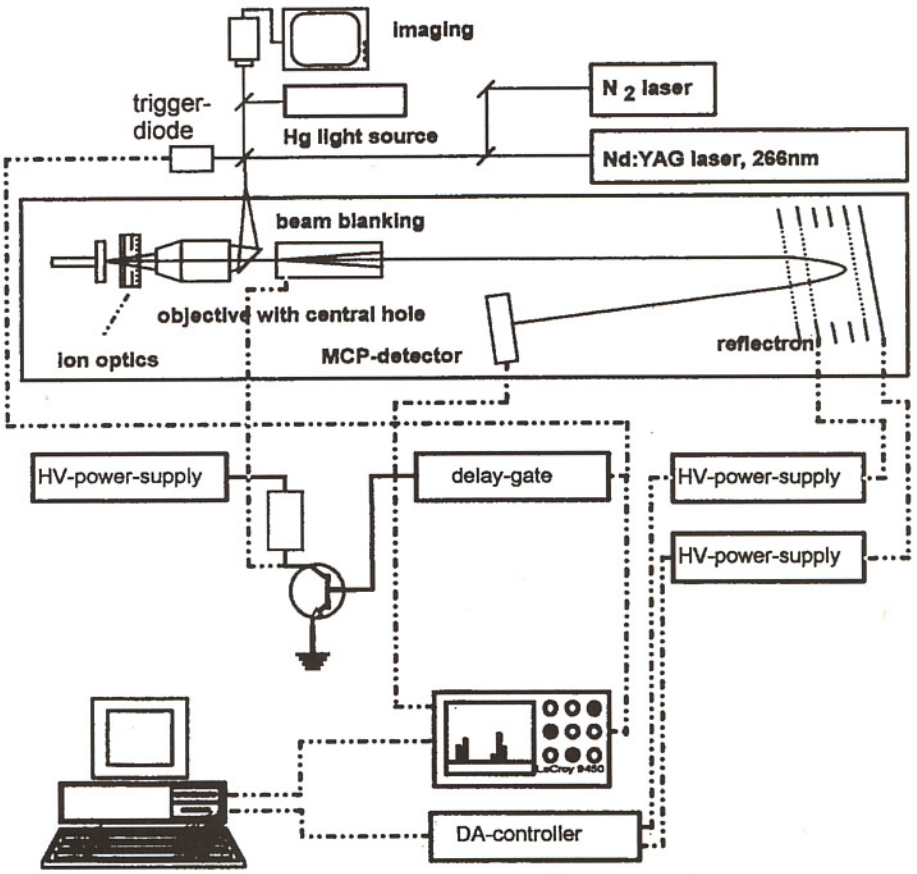

Fig. 2. Schematic setup of MALDI-RETOF-MS.

beam blanking and precursor ion selecting device is located. Precursor mass selectivity with this simple device is about 1 : 50 which is good enough to separate e.g. $(M + H)^+$ from $(M + Na)^+$ precursor ions for 1000 u parent molecules. It should be kept in mind that, in MALDI, the yield of prompt fragments is extremely low. Thus, precursor selection with parent molecules > 1000 u is needed only in heterogeneous samples (mixture analysis) with multiple precursors within about the same mass range.

SIMION (D.A. Dahl and J.E. Delmore, EG&G Inc, Idaho) trajectory modelling indicate that the complete arrangement transmits ions within a ±60° take off angle under the conditions that: (1) the lateral kinetic energies of the ions do not exceed 2×10^{-3} of the forward component (e.g. 20 eV at 10 kV acceleration voltage); (2) the aspect ratio (length to diameter) of the central extraction tube through the focussing optics is about 30; (3) off-axis misalignments are carefully avoided.

It was found that the arrangement not only helps to bring mass resolution of the instrument (for parent molecules up to ≈ 3000 u) close to its theoretical limit ($M/\Delta M \approx 5000$), but, acting as a kind of space filter element, the whole device has the further advantages of feeding the TOF spectrometer with a fairly well collimated ion beam (divergence limit about ±1.5°) and of preventing most of the unwanted particles (early neutrals, decay products formed during acceleration, stray- or secondary particles) from reaching the spectrometer.

Standard conditions for ion extraction were an acceleration voltage ≈ 10 kV and an initial extraction field strength $\approx 3 \times 10^4$ V cm^{-1}, unless otherwise indicated.

TOF-spectrometer and reflectron

The geometrical scheme of the TOF reflectron-MS is illustrated in Fig. 3. Here, s designates the acceleration distance over which ions are acquiring their drift energy E_d. The split extraction field allows the adjustment of the initial field strength (E_i) independently of the total acceleration voltage applied. L_1 is the length (2034 mm) of the field free drift path up to the entrance of the reflectron, d_1 (20 mm) and d_2 (239 mm) the length of the first and the second retardation field respectively of the reflectron, and L_2 (1228 mm) the second field free drift path between reflectron and the large-area MCP detector (72 mm diameter).

In Fig. 3 ion flight paths of either parent or fragment ions illustrate the way in which a reflectron distinguishes between masses of isovelocic fragment ions by flight time dispersion. Fragment ions produced in the first field free drift path have the same velocity as their parents, and, hence, enter the reflectron all at the same time but with different kinetic energies. The kinetic energy (E_f) of a fragment ion is given by

$$E_f = E_p f_m \qquad (f_m = m_f/m_p) \tag{1}$$

where E_p is the kinetic energy of the precursor ion and m_p and m_f are the masses of the precursor and fragment ion respectively. Since fragment ions do not penetrate into the retarding field of the reflectron as deeply as their parents, their turn-around time is shorter. Hence, they leave the reflectron earlier and arrive sooner at the detector than their unfragmented precursors.

For a single-stage reflectron with a homogeneous deceleration field a simple linear relationship exists between the flight times (t_p and t_f) and the masses (m_p and m_f) of the precursor and fragment ions respectively:

$$2(t_f/t_p) = (m_f/m_p) + 1 \tag{2}$$

Thus, in principle, a complete mass spectrum of fragment ions can be simultaneously recorded by employing a single-stage reflectron in its usual mode of operation [19,20]. The problem here is mass resolution. In all kinds of reflectrons optimal time focussing of ions with an initial energy spread requires that ions spend a certain time in the reflectron. If this focussing condition is mismatched because the passage through the reflectron is either too long or too short, mass resolution is more degraded, the more the actual ion flight path (or

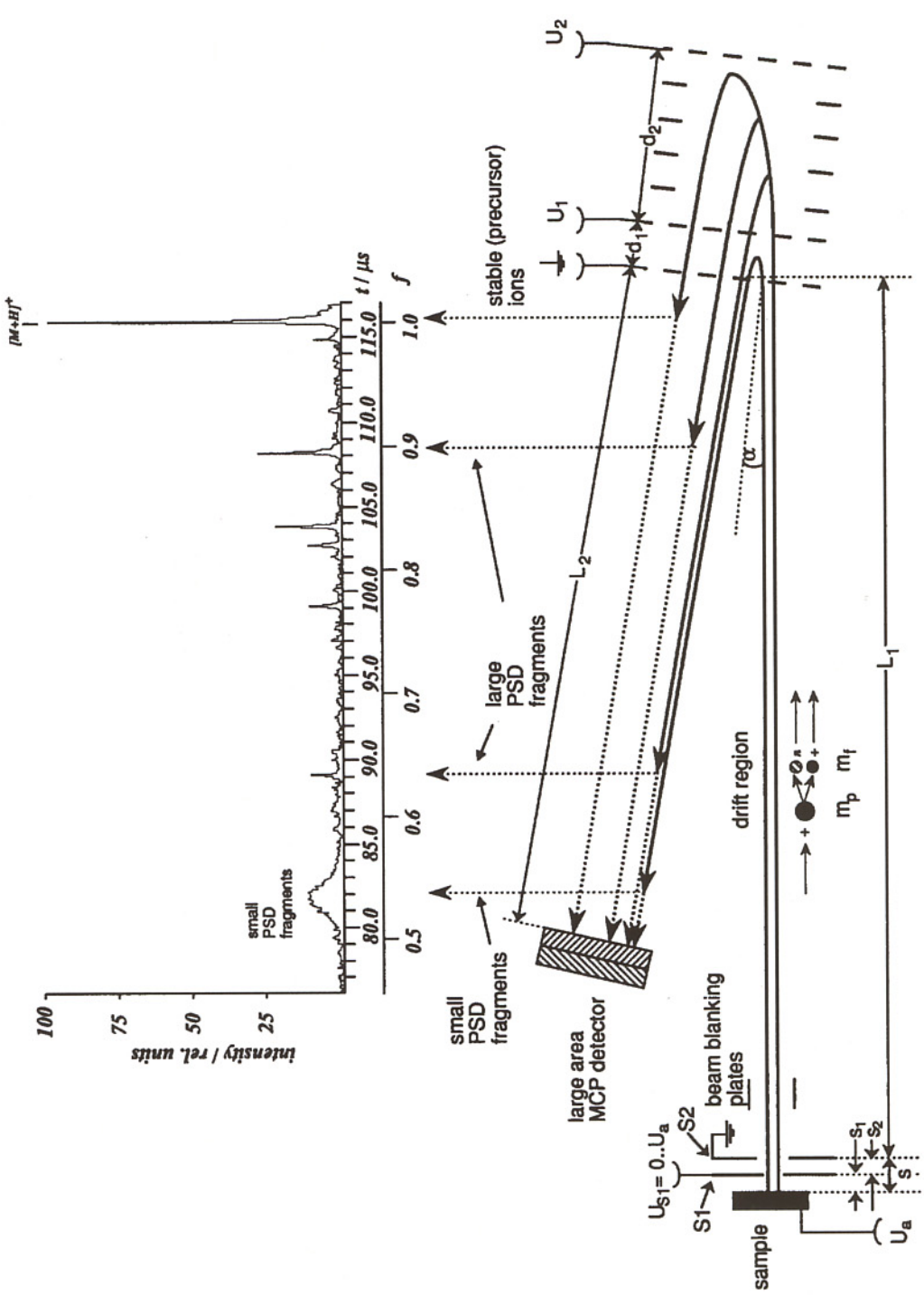

Fig. 3. Schematic illustration of fragment ion mass spectrometry in a two-stage reflectron TOF-MS ($s_1 = 4$ mm, $s_2 = 4$ mm, $L_1 = 2034$ mm, $d_1 = 20$ mm, $d_2 = 239$ mm, $L_2 = 1228$ mm).

flight time) in the reflectron deviates from optimal conditions. Therefore, the recording of a complete fragment ion mass spectrum with acceptable mass resolution requires many consecutive "tuning" steps of the reflectron voltages in order to match optimal time focussing conditions for any (small) segment of the full daughter ion mass range recorded.

As illustrated in Fig. 4 a two-stage reflectron is less feasible against deviations from the optimal penetration depth or optimal residence time than its single-stage counterpart [21]. In an optimally designed device, conditions can be found where the window of daughter ion energy (or mass), over which flight time focussing (i.e. $\Delta T/T$ of fragment ions) would not exceed say 2×10^{-4} can be made as wide as one fifth of the full fragment ion energy (or mass) range, whereas a single-stage reflectron, for the same resolution, would allow the accommodation of only a mass segment of 0.09 full scale. Consequently, in a two-stage reflectron operated e.g. at voltages set for optimal mass resolution of 12 keV precursor ions ($U_1 = 7162$ V, $U_2 = 12.500$ V in our case), the first segment of fragment ion energies or masses over which ions will be recorded with an acceptable resolution of say 4×10^{-4}, is 8000 eV $< E_f(m_f) <$ 11 000 eV, i.e.

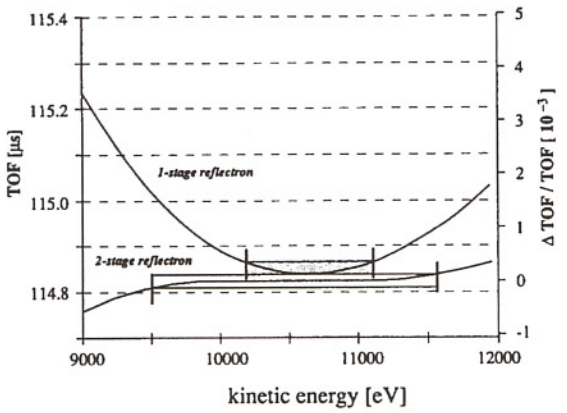

Fig. 4. Comparison of ion flight time as dependent on kinetic energy in a RETOF MS equipped with either a single-stage or a two-stage reflectron. Calculation is based on the geometrical and electrical parameters applied in the actual RETOF configuration assuming a parent ion of 1350 u. Parameters for the single-stage reflectron were adjusted to the same virtual flight path.

one quarter of the full fragment ion mass scale. Also, fragment ions with 5800eV $< E_f(m_f) <$ 7000 eV or 11 000 eV$< E_f <$ 12.000 eV will still be distinguishable but with increasingly poorer mass resolution. All other fragment ions with $E_f(m_f) <$ 7162 eV will not penetrate into the second stage of the reflectron but will be mirrored by the short first stage with virtually no mass dispersion at all (see inset to Fig. 3).

In order to obtain full mass spectra of PSD fragment ions with a two-stage reflectron, typically 10 to 14 consecutive mass scale segments must be recorded with the reflectron adjusted to the respective fragment ion energies. This approach gives sufficient segment overlap to compile complete fragment ion mass spectra at optimal mass resolution.

Mass calibration of fragment ions

While, in a single-stage reflectron TOF-MS, a simple relationship exists between the flight time and the mass of a fragment ion (see above), mass calibration of fragment ions dispersed in a two-stage reflectron is anything but straightforward, since the full motion equation describing the flight time in the reflectron cannot be solved in terms of fragment ion mass. Therefore, if one wants to avoid tedious calibrating procedures via model metastables of known precursor and daughter masses, one needs to know, to the highest possible accuracy, the geometrical parameters of the spectrometer as well as the actual (variable) voltage settings applied. Based on this set of data and the actual flight times of the fragment ions recorded, a computer can calculate by iteration the fragment ion masses with the desired accuracy.

The motion equation of the RETOF-MS in its general form can be written as

$$T_f = [t_a(s_a, U_a, m_p), + t_d(L_1, L_2, \alpha, U_a, m_p) + t_r(d_1, d_2, \alpha, U_a, U_1, U_2, m_p, f_m)] \quad (3)$$

where: T_f = total flight time of the fragment ion (m); t_a = flight time in the acceleration region(v); t_d = flight time in the field free drift region (v);

t_r = flight time in the reflectron (v); m_p = mass of the precursor ion (v); s_a = length of the acceleration region (f); U_a = acceleration voltage (v); L_1 and L_2 = first and second field-free drift length (f); α = half angle of deflection of the ion flight path versus the sample surface normal (f); d_1 and d_2 = length of the first and the second stage of the reflectron (f); U_1 and U_2 = applied voltages at grid 2 and 3 of the reflectron relative to the flight tube potential (v); f_m = fragment/precursor mass ratio (c). In the preceding list (f) indicates a fixed (instrumental) parameter, (v) an experimental variable, (m) a measured variable and (c) a parameter to be determined.

For practical work, an algorithm based on the above set of parameters has been integrated into the PC-based "Ulisses" TOF data acquisition program (Chips at work, Bonn, Germany) to perform this task.

As will be shown in the Results section the average mass resolution of fragment ions is mainly determined by the width of the precursor ion signal and reaches typically $M/\Delta M \approx 800$–1000 (FWHM) if precursors are in the 1000–2000 u range (see example given in Fig. 7).

Detector and signal recording

One of the inherent problems of using a reflectron for PSD fragment ion mass discrimination relates to the fact that fragment ions of different masses are also laterally dispersed by the reflectron at least if — as is usually the case — the reflectron axis deviates from a 180° reflection angle by a few degrees (2–3° vertically in our case). Thus, if one wants to avoid mass dependent transmission losses, a large area detector is mandatory. Under our actual geometrical conditions we found a 75 mm diameter MCP detector to represent just the lowest theoretical area limit which would accommodate the lateral (geometrical) spread of fragment ions recorded over a typical mass scale segment. We are, however, fairly sure that, owing to collisional momentum transfer and kinetic energy release, the angular spread of fragment ions is by far larger than the spread based simply on geometrical calculations.

To avoid postacceleration by fringe fields extending from the front side of the detector (usually at −1.8 kV), a grounded grid was placed about 15 mm in front of the first channel plate, or the MCP detector was offset such as to shift its front-side potential to zero. While the latter procedure is certainly preferable with respect to correct mass assignment of, in particular, low mass fragment ions, the former prevents sensitivity loss (very low kinetic energies) for these ions.

Usually 50–100 spectra were summed for each voltage setting (mass window) at a cycle frequency of 1 Hz. No smoothing or filtering routine was applied to the spectra presented in this paper.

This means that recording of a full sequence spectrum with typically 10–12 overlapping spectral segments requires ≈ 30 min of recording time in our actual setup.

Results

State of the art performances: a model case (Substance P)

This paragraph aims to demonstrate the instrumental performances reached so far. Since PSD-RETOF mass spectrometry for peptide sequencing after MALDI is an innovative approach not yet common to, or established amongst, mass spectrometrists we start with a model case to illustrate conditions and achievements in detail.

As a model peptide we have chosen Substance P, a neuropeptide (monoisotopic mass 1346.7 u) consisting of 11 amino acid residues which has been frequently and extensively investigated in high energy as well as in low energy CAD MS-MS studies [5,6,27–29]. Substance P was also included in the pioneering work of Tang and co-workers [19,20] on the application of reflectron (single-stage) TOF mass spectrometry to analyse either metastable or prompt product ions after particle induced desorption and was the subject of a recent attempt to explore multiphoton photoionization-dissociation (MUPI) for peptide sequencing [30].

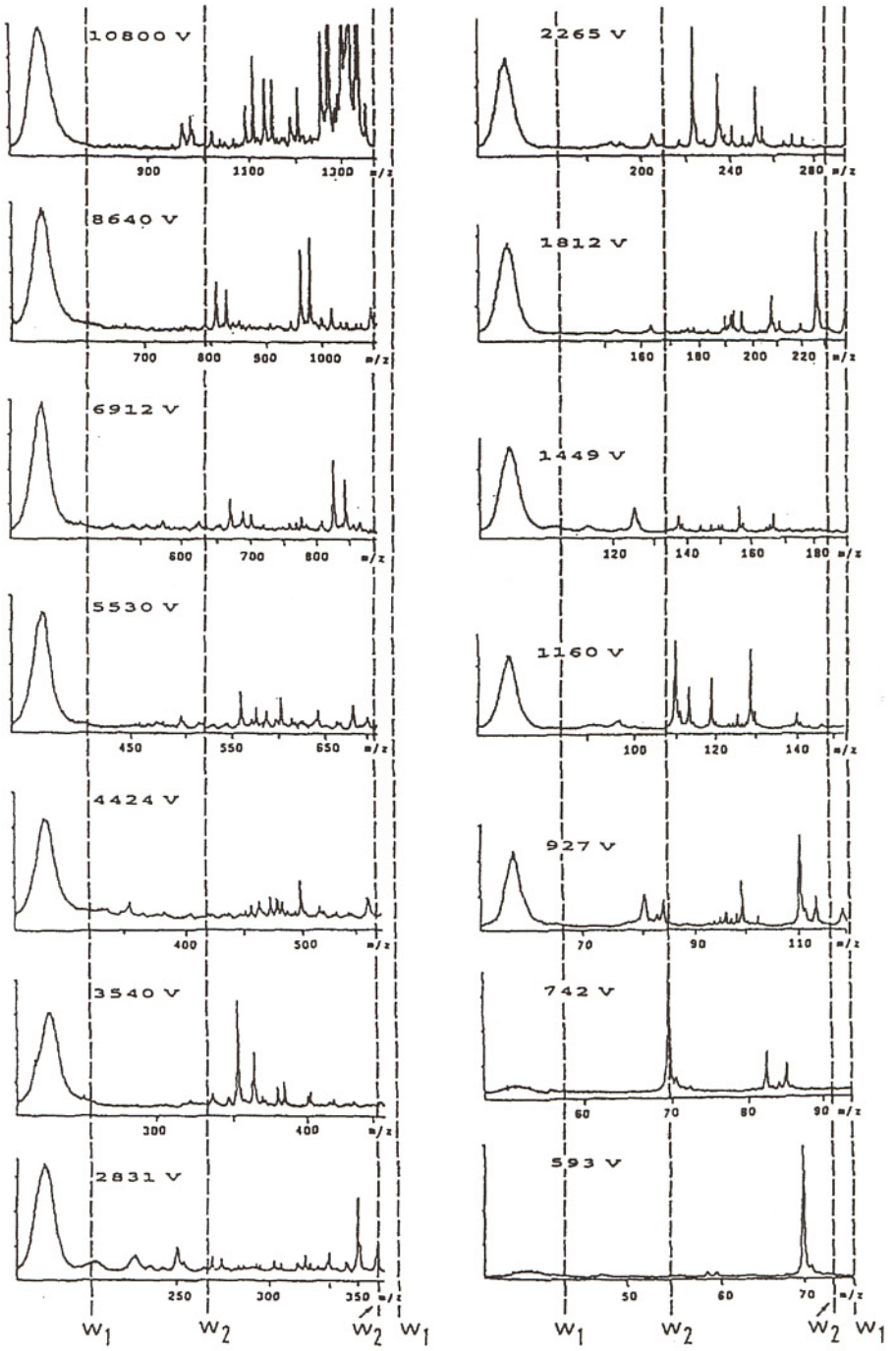

Fig. 5. Consecutive segments of PSD fragment ion spectra of Substance P. Labels in each spectrum indicate the voltage settings of U_2 in the two-stage reflectron with $U_1 = 0.57377\,U_2$. See text for a further explanation.

PSD ion spectra recording

Figure 5 contains a series of consecutive PSD fragment ion segment spectra obtained from Substance P in a DHB matrix after laser desorption ($\lambda = 337$ nm). On the left hand side each segment spectrum starts with a broad peak containing all those fragment ions which, at the indicated retarding field, have not penetrated the second stage of the reflectron and have been mirrored by the first stage without mass dispersion. This "junk-hill" is a fair indicator of the total fragment ion yield (about 50% of unfragmented parent molecules in the case of Substance P) and helps to roughly scale fragment ion peak amplitudes within a series of consecutive segment spectra. On the right hand side of the "junk hill" each segment spectrum displays a number of mass resolved fragment ion signals. Each spectrum might be visualised as part of a string which, moving left to right through a window, is being continuously pulled out of the "junk hill" when the reflectron voltages are reduced from standard settings (upper left hand panel) down to the lowest values (lower right hand panel). Since useful sequence information is not expected from ions smaller than 70 u, recording was usually terminated with the last spectrum tuned to the appropriate mass scale segment.

The spectral window over which mass separated fragment ion signals can, in principle, be identified is indicated by two broken vertical lines (w_1) in Fig. 5. They delineate borders given by the foot of the "junk hill" on the left side and, on the right side, by a point where fragment ions start to disappear (because they are leaving the reflectron on the rear side). The mass range of each segment spectrum extends over a range of 0.56 to 1 of the largest fragment ion (m_{fl}) accommodated. This means that, basically, five consecutive segment spectra recordings could cover the whole product ion mass range extending from the precursor ion mass (m_p) down to say $0.07\,m_p$. Since, however, acceptable mass resolution is obtained only in a smaller spectral window which extends from say $0.7\,m_{fl}$ to $0.9\,m_{fl}$ (indicated by the borders labelled w_2), 10–14 segment spectra are usually needed for full mass range analysis.

Complete PSD fragment ion mass spectra, as shown in Fig. 6, are composed of a series of consecutive overlapping cut outs from segment spectra as displayed in Fig. 5. Such composed spectra are infected with the problem of fitting a mass scale on the abscissa since, in a two-stage RETOF, the relationship between time of flight and fragment ion mass neither follows a simple steady function nor does the same expansion factor apply for each segment. Thus, in the absence of an available rescaling algorithm, the fragment ion signals of the spectra displayed in this work are individually mass assigned.

Accuracy and precision, and lower limit of analysis

In the model case of Substance P, fragment ion mass assignments and cleavage interpretations according to the scheme of Roepsdorf and Fohlman, and Johnson et al. [31] are given in Table 2 and Fig. 6. Fragment ion mass resolution $M/\Delta M$ (FWHM) is in the range of 800 to 1200 (see also Fig. 7) which is typical for precursors the size of Substance P. Accuracy of mass assignments is 5×10^{-4} (averaged over the whole fragment ion mass range) with slightly better figures (3×10^{-4}) applying for fragment ion masses above 700 u (relative errors in the digital control of reflectron voltages are larger at lower absolute voltage settings). Precision within one experiment done on the same sample is about 2×10^{-4} and worsens to $3\text{–}4 \times 10^{-4}$ on a day to day basis.

With 60 single spectra summed for each mass segment, the signal-to-noise ratio is excellent in cases like Substance P (no filtering or smoothing was applied to the spectra shown). The total yield of fragment ions in this particular case was about 0.5 with respect to the precursor ions reaching the detector unfragmented. (For a discussion on efficiency of fragmentation dependent on various experimental parameters, see the mechanisms of activation and energy transfer below.

The amount of analyte consumed is never known

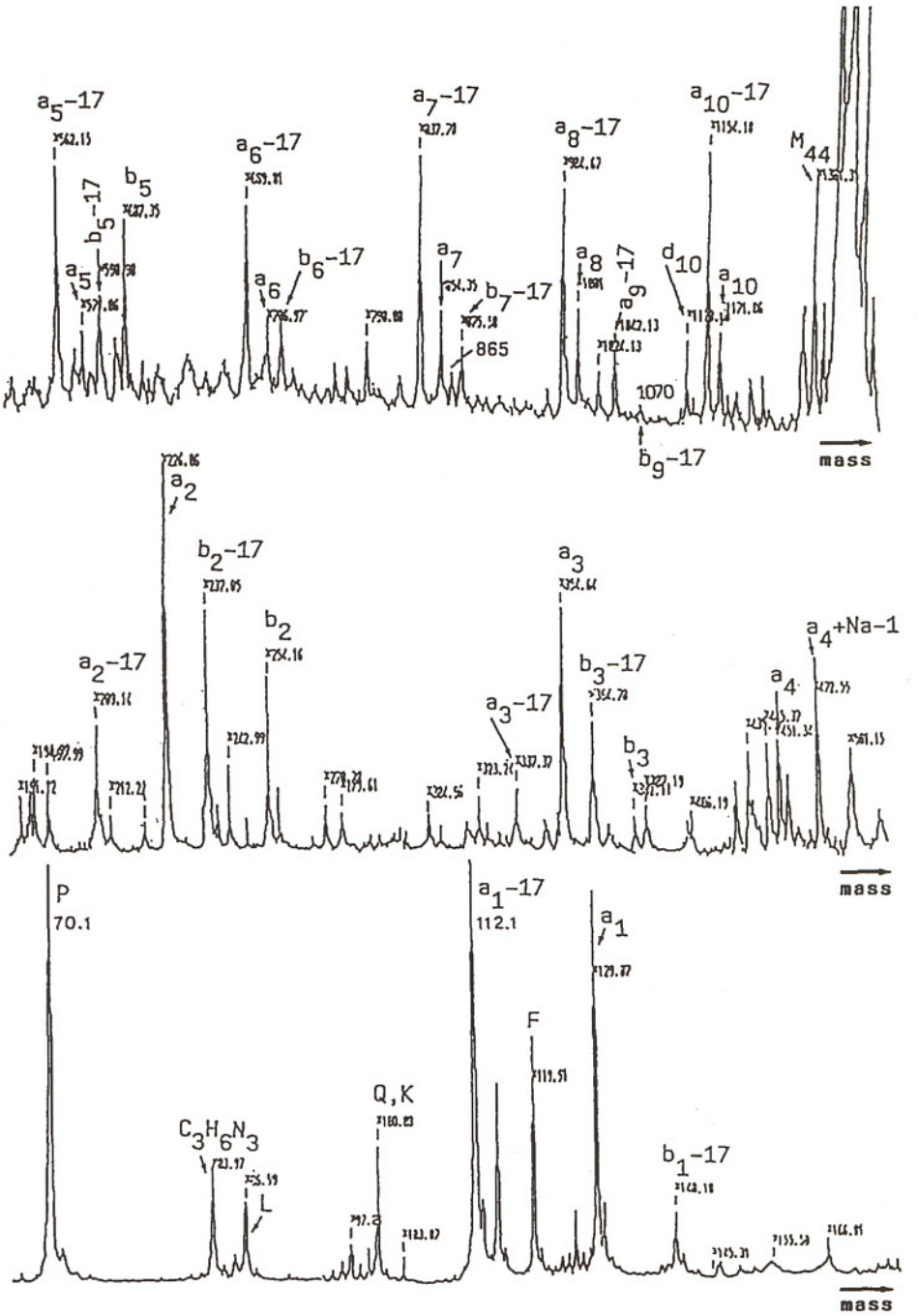

Fig. 6. Complete PSD fragment ion spectrum of Substance P (1347.7 u). This is a composed spectrum consisting of 14 segments taken from recordings as shown in Fig. 5. For each segment 50 single shot spectra were summed up. Mass labels are those which the computer program calculated on the basis of geometrical data and actual voltage settings. Total acceleration voltage = 10 kV; initial acceleration field strength $\approx 3 \times 10^4$ V cm^{-1}.

Table 2
Calculated and observed masses of PSD fragment ion of Substance P

Peak No.	Fragment mass		ΔM (u)	Accuracy (10^{-3})	Assignment
	Calc.	Obs.			
1	1302.7	1302.1	−0.6	0.46	$M-44$
2	1171.7	1171.9	−0.2	0.17	a_{10}
3	**1154.2**	**1154.2**	**−0.5**	**0.43**	**$a_{10}-17$**
4	1029.4	1028.6	0.8	0.80	d_{10}
5	1041.6	1042.1	−0.5	0.50	a_9-17
6	1001.6	1001.4	−0.2	0.20	a_8
7	**984.6**	**984.7**	**−0.1**	**0.10**	**a_8-17**
8	876.5	875.8	−0.7	0.80	a_7+Na-1
9	854.5	854.4	−0.1	0.12	a_7
10	**837.5**	**837.7**	**+0.2**	**0.24**	**a_7-17**
11	718.5	718.3	−0.2	0.27	b_6-17
12	707.4	707.0	−0.4	0.57	a_6
13	**690.4**	**689.8**	**−0.6**	**0.86**	**a_6-17**
14	**607.4**	**607.3**	**+0.1**	**0.16**	**b_5**
15	590.4	590.9	+0.5	0.84	b_5-17
16	579.4	579.1	−0.3	0.51	a_5
17	**562.4**	**562.2**	**−0.2**	**0.36**	**a_5-17**
18	**473.4**	**472.9**	**−0.5**	**1.06**	**a_4+Na-1**
19	451.3	451.3			a_4
20	382.3	382.2	−0.1	0.26	b_3
21	365.3	364.8	−0.5	1.37	b_3-17
22	**354.3**	**354.6**	**+0.3**	**0.85**	**a_3**
23	337.3	337.4	+0.1	0.30	a_3-17
24	254.2	254.2			b_2
25	**237.2**	**237.1**	**−0.1**	**0.42**	**b_2-17**
26	**226.2**	**226.1**	**−0.1**	**0.44**	**a_2**
27	209.2	209.1	−0.1	0.48	a_2-17
28	140.1	140.1			b_1-17
29	**129.1**	**129.1**			**a_1**
30	**120.1**	**119.9**	**−0.2**	**1.60**	**(Phe)**
31	**112.1**	**112.1**			**a_1-17**
32	101.1	100.9	−0.2	2.00	(Lys/Glu)
33	87.1	87.0	−0.1	1.10	(Leu)
34	84.1	84.0	−0.1	1.20	$C_3H_6N_3$
35	**70.1**	**70.1**			**(Pro)**

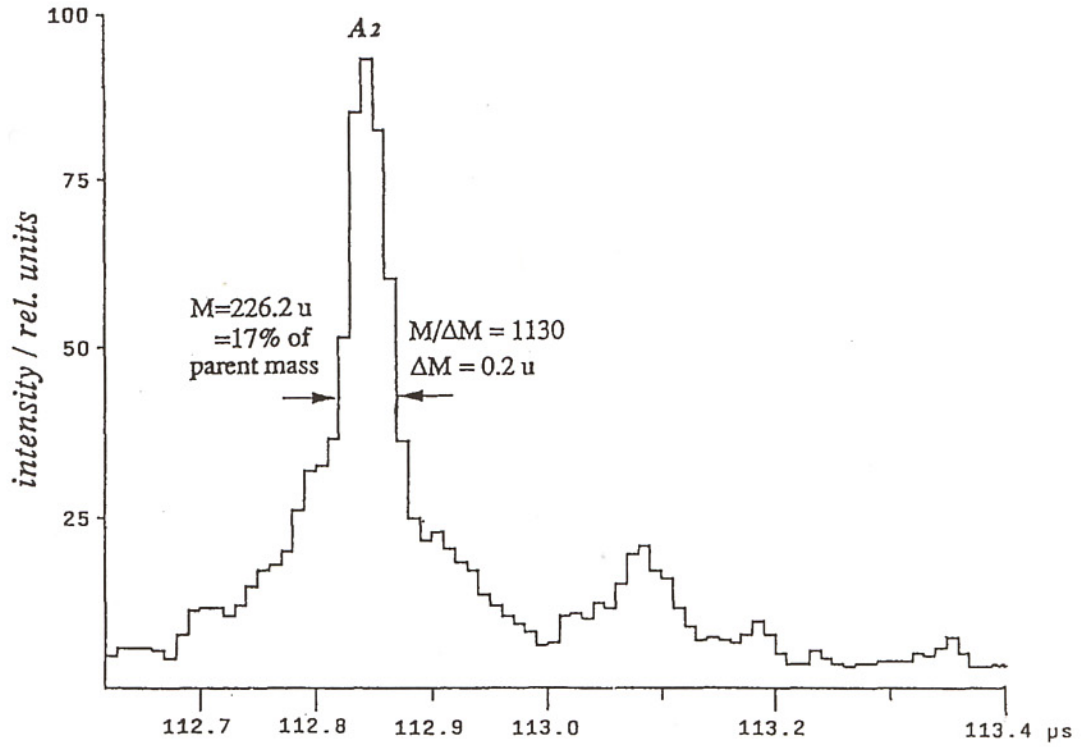

Fig. 7. PSD fragment ion mass resolution demonstrated for the a_2 fragment of Substance P (full width at half maximum definition). Matrix was DHB, $\lambda = 337$ nm, $U_{acc} = 10$ kV.

exactly in MALDI but can be approximated (from data such as the diameter of the laser focus, the amount of sample deposited per unit area, and the number of laser shots needed to exhaust one sample position) to a value in the range 20–40 amol per laser shot under the present conditions. Hence, with 1000 laser shots for complete fragment ion analysis, analyte consumption amounts to 20–40 fmol. This figure is certainly not the lower limit for analysis. As the example in Fig. 8 demonstrates, signal-to-noise ratio would have permitted a reduction in the number of spectra summed in Fig. 6 by at least one order of magnitude without loss of essential information. Thus, the question of detection limits lends itself to the problem of how sample preparation protocols can be devised to match such ultra-low detection capabilities. It is obvious that the way samples are usually prepared for MALDI-TOF mass spectrometry are unsatisfactory. However, with the foreseeable adaptations of MALDI-TOF mass spectrometry to ultra-small volume separation techniques such as capillary zone electrophoresis, instrumental sensitivity will certainly be greatly improved.

Product ion pattern and type of cleavages

As to the pattern of favoured backbone cleavages, there are some similarities but also some remarkable differences between PSD-RETOF and CAD-MS-MS for which the example of Substance P appears to be already fairly representative.

First of all there is the near complete absence of side chain specific cleavages (d_n in the case of Substance P) in contrast to high energy CAD spectra which regularly contain almost all possible d_n fragments at yields comparable to, or even exceeding, those of the corresponding a_n fragments. However, high energy CAD spectra of Substance P are usually free of b_n fragments [28,29] in contrast to low energy CAD spectra obtained in triple quad or hybrid setups which are largely dominated by b_n

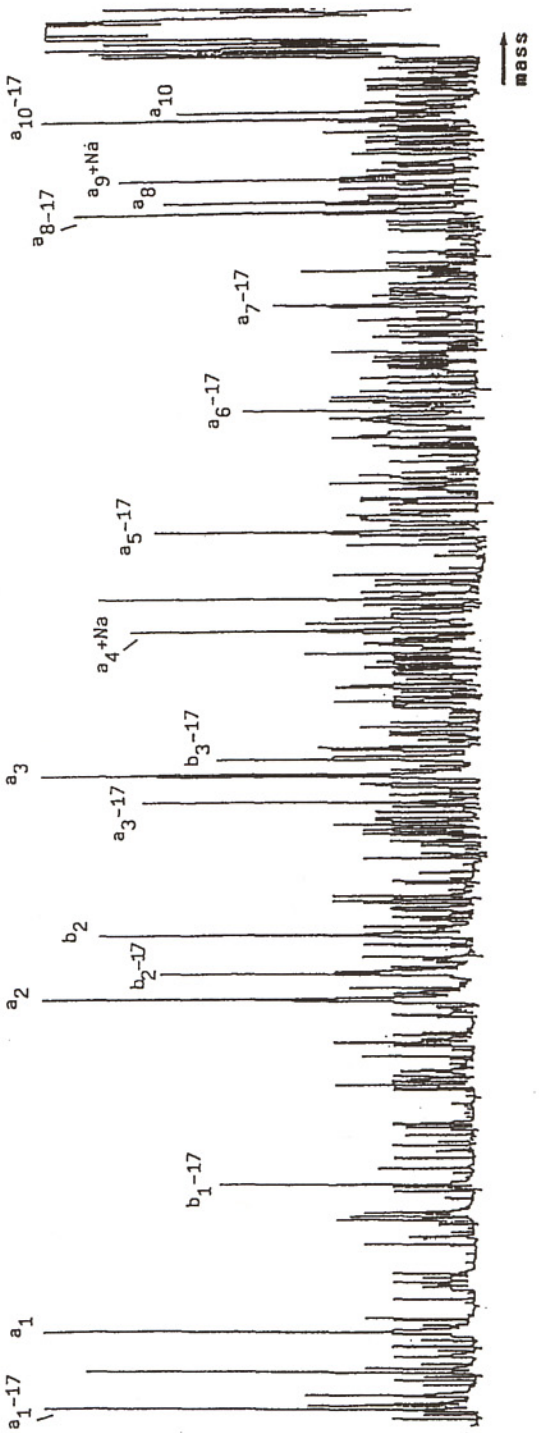

Fig. 8. Ten segment single shot PSD fragment ion spectrum of Substance P. Total amount of sample consumed ≈ 400 amol.

fragments [5,6]. MALDI-PSD-RETOF mass spectra apparently represent some intermediate situation featuring both a complete a_n and a nearly complete ($n = 1$–9) b_n series together. (These findings will be reconsidered and further discussed below in the Mechanisms of activation and energy transfer section).

Another obvious peculiarity of our MALDI-PSD fragment ion spectra is the predominance of the $(a_n - 17)$ and $(b_n - 17)$ signals which usually occur at much larger abundances than the corresponding a_n and b_n counterparts. The formation of these products is usually thought to be due to ammonia loss from an N-terminal arginine residue. Although such satellites are not uncommon in CAD spectra they never reach yields as observed under the present conditions. We cannot exclude the possibility that a small fraction of our prompt precursor ions are already desaminated, although such ions have never been found in the prompt MALDI spectra recorded by linear TOF instruments. Since precursor ion selection in our actual instrument does not yet allow discrimination between MH^+ and $(M-17)H^+$ species at 1348 u (Substance P) we must leave this question open for now. However, the only other experimental condition under which $(a_n/b_n - 17)$ satellites of comparable intensity have been observed is reported in the work of Tang et al. [20] on PSD-RETOF spectra after particle induced desorption

Table 3
Comparative performance data obtained in MS-MS studies of Substance P

Mass spectrometer			Fragment mass accuracy (u)	Peak half width (u)	Predominant backbone cleavages	Estimated limits of analysis	Ref.
Type of device	Ion source	Activation mechanism					
Four-sector BEEB	FAB 35 keV cesium	High energy CAD (10 keV) helium	±0.3	0.3	a_n, d_n	15 pmol	[5]
Hybrid BEqQ	FAB 8 keV xenon	Low energy CAD (14–27 eV) argon	±0.5[a]	3.0	a_n, b_n	370 pmol	[5]
Four-sector	CF-FAB	High energy CAD	±0.3	0.3	a_n, (d_n)	200 fmol	[27]
Four-sector EBEB	FAB 8 keV xenon	High energy CAD (6 keV) helium	±0.3[a]	0.3[a]	a_n, d_n	100 pmol	[6]
Four-sector EBEB	FAB 8 keV xenon	High energy CAD (4 keV) helium/argon	±0.3	0.3[a]	a_n, d_n (He) a_n, d_n (Ar)	Not determined	[28]
Four-sector EBEB	FAB 6 keV xenon	High energy CAD (5 keV) helium	±0.3	0.2 at 225 u	a_n, d_n	0.5 pmol	[29]
RETOF one stage (ion count. m.)	SI 10 keV cesium	PSD (8 keV)	±0.3	0.2	a_n, $a_n - 17$ b_n, $b_n - 17$	0.1-1 pmol	[19]
RETOF one stage (ion count. m.)	SI 10 keV cesium	Prompt decay	±0.3	0.2	a_n	0.1-1 pmol	[20]
RETOF two stage (analogue m.)	MALDI (DHB/ 337 nm)	PSD 10 keV	±0.3	0.2	$a_n - 17$, a_n (PSD) $b_n - 17$, b_n a_n, d_n (CAD)	0.4-4 fmol	This work
RETOF two stage (analogue m.)	LD/MUPI	Prompt Photo-dissociation	±0.3	0.3	z_n, y_n, x_n (a_n, c_n)	Not determined	[30]

[a] Estimated from published data.

of Substance P. It is interesting to note that prompt (SIMS) fragment ions obtained under essentially the same conditions did not contain such satellites at all.

Thus, for the time being, we conclude that loss of ammonia is primarily a secondary (PSD) process which, due to a relatively low rate constant, requires a rather long time window to reach that yield which is obtained under our conditions. This type of cleavage seems to run in parallel with the backbone fragmentation processes and, to a lesser extent, also occurs in peptides containing: (1) either arginine in non-terminal positions or (2) aminated side chains other than arginine.

Comparison with MS–MS

From the viewpoint of practical mass spectrometry it is necessary to compare these results with those obtained by MS-MS. In a recent study, Bean et al. [5] have investigated the performance of four-sector instruments (BEEB) versus hybrid designs (BEqQ) in the analysis of collisionally activated peptide fragment ions including Substance P. Their data appear to be representative of the many other CAD investigations carried out on this frequently used model peptide (refs. 6 and 27–29). Table 3 summarises most of the relevant data collected from the literature. It demonstrates that, at this point, MALDI-TOF mass spectrometry of PSD product ions can already easily compete with standard MS-MS. Accuracy and precision of mass assignment, mass resolution, and (although not explored in Table 3) time of analysis, all reach the performance of four-sector tandem instruments equipped with an array detector [29]. Instrumental sensitivity in PSD-RETOF analysis is better by at least two orders of magnitude; the upper precursor mass limit (see next paragraph), up to which full sequence information can be obtained, is about 2500 to 3000 u.

General observations

Our actual experience with PSD fragment ion analysis of peptides extends over about 60 compounds (conjugates included) ranging from Leu-enkephalin (five residues, 556 u) to ACTH (39 residues, 4567 u). Table 4 lists some of the investigated peptides larger than 1000 u which gave full sequence spectra, with the exception of apamine internally crosslinked by two disulphide bonds.

Table 4
List of peptides investigated

Substance		Average mass (u)	Amino acid sequence
Synthetic peptides	I	1030.3	H-GAKAVGEAKAAG-OH
	II	1085.3	. -L . . . . . G- . .
	III	1085.3	. -G . . . . . L- . .
	IV	1043.3	. -G . . . . . A- . .
	V	1071.3	. -G . . . . . V- . .
Renin-inhibitor		1156.4	H-PHPFHLFVY-OH
# 421		1184.6	H-IGEGTYGVVYK-OH
Substance P		1347.7	H-RPKPQQFFGLM-NH_2
Tyr_8-Substance P		1363.7	H-RPKPQQFYGLM-NH_2
# 435		1545.8	AC-RKSATTKKVASSGSP-NH_2
Gamma-MSH		1570.8	H-YVMGHFRWDRFG-OH
Bombesin		1619.9	H-XQRLGNQWAVGHLA-NH_2
# 520		1668.9	H-QRKEAADPLASKLNK-OH
Tyr_4-Bombesin		1669.9	H-XQRYGNQWAVGHLA-NH_2
# 493 (Lipid)		1864.1	Fatty acid-GLTISSLFSRLFGKK-OH
Apamin		2021.5	H-CNCKAPETALCARRCQQH-NH_2
Melittin		2846.6	H-GIGAVLKVLTTGLPALISWIKRKRQQ-NH_2

The largest peptide which gave a full set of identifiable sequence ions was melittin (26 residues, 2849 u). Figure 9 shows a typical spectrum.

There are a few recent reports on attempts to fragment melittin by ESI in combination with either a four-sector instrument [32], a triple quad [16], or an ion-trap MS-MS device [15]. While the instrumental conditions of these approaches differ in many respects they share multiple low energy collisions as a common denominator for precursor ion (pre)excitation. These attempts have been partly successful insofar as they could produce comparable product ion spectra of melittin (4+ or 2+) precursors which, in the absence of product ion charge state information and with the rather limited mass resolution attained, could only tentatively be assigned to at least some partial series of y- and b-type sequence ions.

Taking those melittin product ion spectra as references we notice that we have certainly got much more complete and unequivocal sequence information with the C-terminal (y, and y−17-type) fragment ion signals dominating the spectrum (two arginine residues near the C-terminus at the 22- and 24-positions). There is, however, also a series of rather abundant b- and a-type fragments, particularly in the low mass region ($n = 2$–8), which, together with the y-type fragments, provide full sequence information on this 26-residue peptide. Although the number of spectra accumulated for each segment in this case had to be increased to $n = 250$ in order to attain an acceptable signal-to-noise ratio, no more than 150 fmol of analyte (out of a sample prepared containing 20 pmol) had to be consumed for the analysis.

The case of melittin, although remarkably successful in principle, can also serve to outline the accuracy limitations inherent so far in MALDI-PSD mass spectrometric analysis. For reasons of optimal yield and "in-source activation" (see below), laser desorption of larger peptides requires irradiances at least 30–50% above the threshold of ion formation. As a consequence, mass resolution drops significantly below the nominal instrumental performance. Thus, isotopic discrimination is usually lost with peptides above say 1800 u and product-ion as well as precursor-ion signals become envelopes of isotopic distribution pattern folded with a T_0 (start time) spread typical for the MALDI ion formation process. Although smoothing and center-of-mass routines can be run on such signals, the degradation of mass assignment cannot be fully offset. In consequence, the factors affecting precision and accuracy of fragment ion mass assignment add up to a typical relative error of $(0.8–1.2) \times 10^{-3}$ for fragment ion masses above 2000 u. This means that, in the present case of the melittin spectrum, mass determination of the larger fragments is within absolute error limits of 1.5–3 u.

Attempts to fragment peptides larger than melittin, e.g. ACTH, gave only limited partial sequence information, usually from the small-sized ($n = 2$–5) and also from a few large-sized products close to the precursor ion mass.

Remarkably enough, the overall efficiency of fragmentation did not diminish with increasing precursor size. From the height of the "junk-hill" relative to the signal amplitude of the unfragmented parent molecule, it even appears that total fragment ion yield increases rather than decreases with larger precursor masses (see Fig. 10). With respect to the increasing number of possible cleavages in such molecules, one might be tempted to see the degradation of the signal-to-noise ratio simply as the consequence of statistics which might be counteracted by accumulating a larger number of spectra. In practice, however, this turned out to be of only limited success. Occasionally, "spectral islands" of fairly-well-discernable signals appeared on top of a "wavy" but otherwise unresolved background which, more or less, extended over all spectral windows. Our actual, but admittedly rather vague, interpretation is based on a conjunction of two phenomena. (1) As already discussed for the example of melittin (see above), mass resolution in MALDI spectra of larger peptides is not as good as one would expect from the instrumental performances. Thus, with the spectral number density of possible cleavages increasing and the isotopic distribution pattern broadening, more and more of the

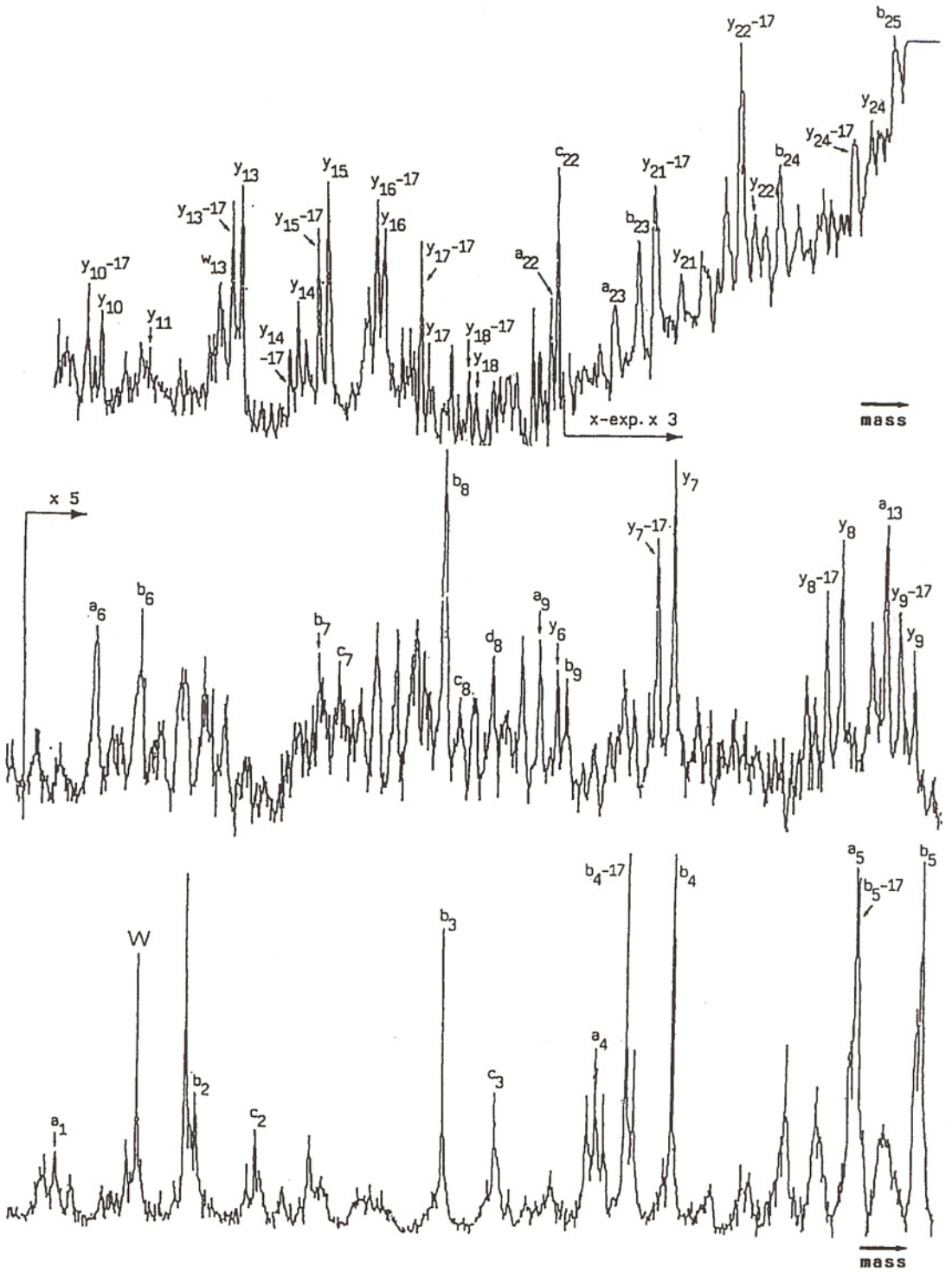

Fig. 9. PSD fragment ion spectrum of melittin (2847 u). Acceleration voltage 12 kV, initial electric field strength $\approx 5 \times 10^4$ V cm^{-1} (250 spectra summed in each of 14 segments).

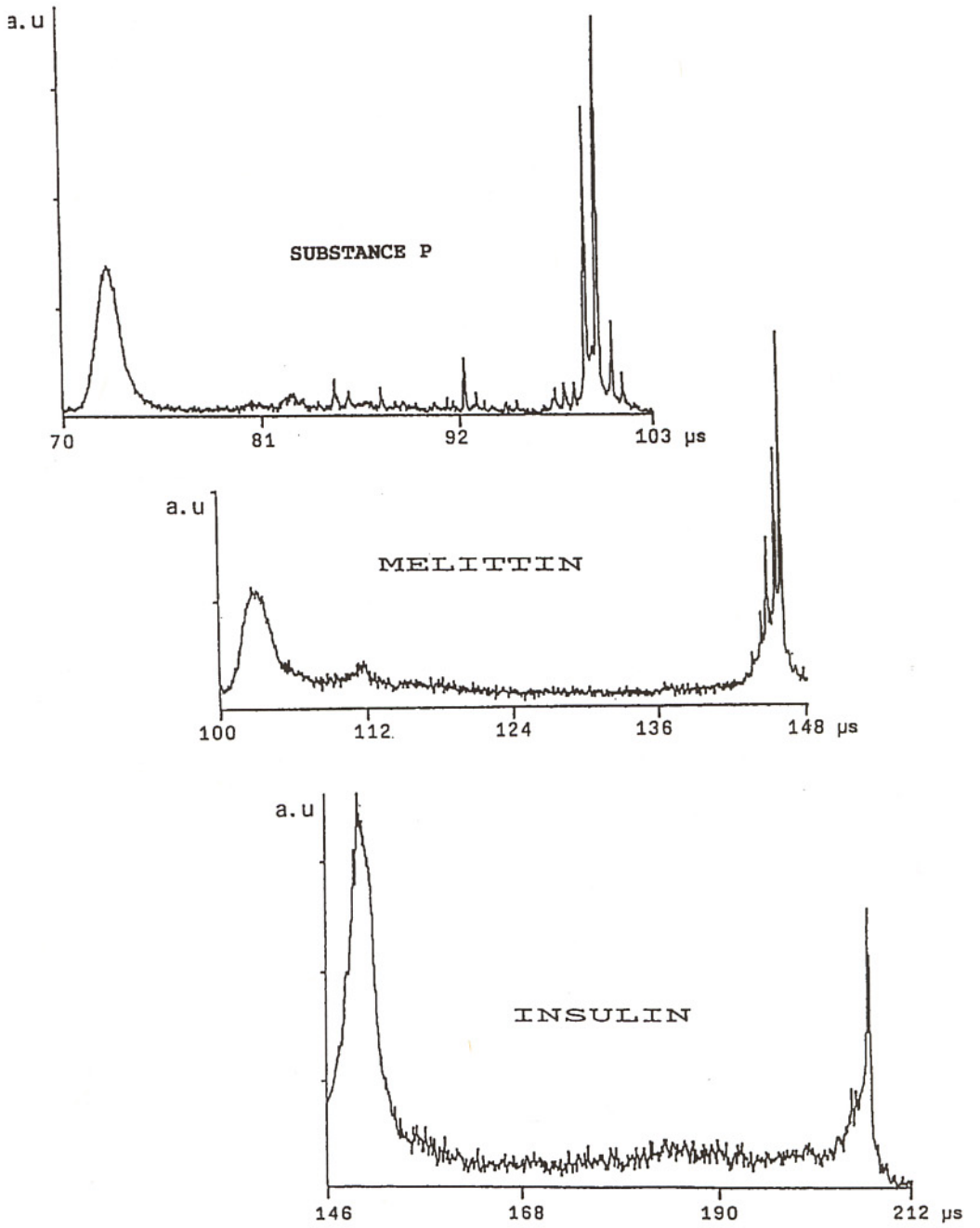

Fig. 10. Increase of total fragment ion yield (compare "junk hill" area versus parent molecule signal amplitude) with increasing precursor ion mass. Spectra were recorded from the same mixed peptide sample. Acceleration voltage was 14 kV, initial field strength $= 4 \times 10^4\ \mathrm{V\,cm^{-1}}$.

smaller signals will smear out in a noisy background. (2) Since, in addition, the rate constants for decomposition are decreasing with larger precursor ion size, the fraction of "late" fragmentations which occur during the residence of an ion in the reflectron or thereafter augments, thereby contributing to an abundant but unresolved fragment ion background.

As to the analogies of PSD with CAD fragment ion spectra, we also observe charge-directed fragmentations, i.e. a predominance of either C- or N-terminal fragment ion series depending on where the charge bearing residues are located. Further congruent findings are: (1) fragment ions ending in a glycine residue appear usually at low abundance, those ending in a proline at high abundance; (2) hydrophobic residues (Leu/Ile and Val) are rather unfavourable while hydrophilic residues (Thr and Ser) are generally more favourable with respect to site directed cleavages.

The presence or absence of very abundant residue-specific immonium ions, in particular those of proline (70 u), threonine (74 u), lysine/glutamine (101 u), histidine (110 u), phenylalanine (120 u), and tyrosine (136 u) is a rather unequivocal indicator for the occurrence or the lack of the corresponding residue, whereas arginine (129 u) and tryptophane (159 u) coincide with b-type fragments of Gly-Ala or Ser-Ala combinations respectively.

We have concentrated our attention primarily on protonated precursors by avoiding alkali contaminated samples or, in cases of minor contaminations, by trying to select the protonated from the cationised (usually Na) species. In a few favourable instances (about equal yields of cationised and protonated precursor species not larger than about 1000 u), where our gated beam blanker permitted a good enough precursor selection, we have tried to compare PSD product ion spectra of both kinds of precursors. The data in Table 5 demonstrate the result of such an attempt in a synthetic peptide (peptide V in Table 4, 12 residues, 1071 u) which had been Na contaminated to such an extent as to yield more than 70% of the precursor ions as catio-

Table 5
PSD fragment ion observed with either $(M + H)^+$ or $(M + Na)^+$ precursor of peptide (V)[a]

$(M + Na)^+$		$(M + H)^+$	
Product mass (m/z)	Assignment	Product mass (m/z)	Assignment
995	$b_{11} + Na + 18$	954	b_{11}
877	$a_{10} + Na - 1$	883	b_{10}
		866	$b_{10} - 17$
		855	a_{10}
		812	b_9
722	$c_8 + Na - 1$	684	b_8
		656	a_8
		627	c_7
635	$b_7 + Na - 1$	613	b_7
607	$a_7 + Na - 1$	585	a_7
478	$a_6 + Na - 1$	484	b_6
		457	a_6
		439	$a_6 - 17$
449	$b_5 + Na - 1$	427	b_5
		399	a_5
328	b_4	328	b_4
311	$b_4 - 17$		
257	b_3	257	b_3
129	b_2	129	b_2

[a] See Table 4.

nised species. While the product ion spectrum of the protonated precursor is dominated by a series of N-terminal b_n and a_n fragments, the product ions of the cationised precursor are mainly of the type (a_n/b_n+Na-1). With cationised precursors, the ladder of sequence ions is terminated by an abundant signal attributed to a product of the type $(b_{11}+Na+18)$. These preliminary results are in agreement with the recent analysis of Teesch et al. [33] employing metastable and CAD fragment ions of gas-phase cationised peptide precursors to investigate the location of the alkali metal in such complexes.

"Internally stabilized" peptides

The presence of internal disulphide, amide, or ester bonds in the investigated peptides is clearly reflected in the pattern of PSD product ions. With the still-preliminary results at hand we can state that such conditions tend to reduce the overall yield of fragment ions in general. In all cases investigated so far, the bond forming residue(s) could easily be located since the series of sequence ions (either N-terminal or C-terminal) usually ended with the fragment next to the stabilised part of the backbone.

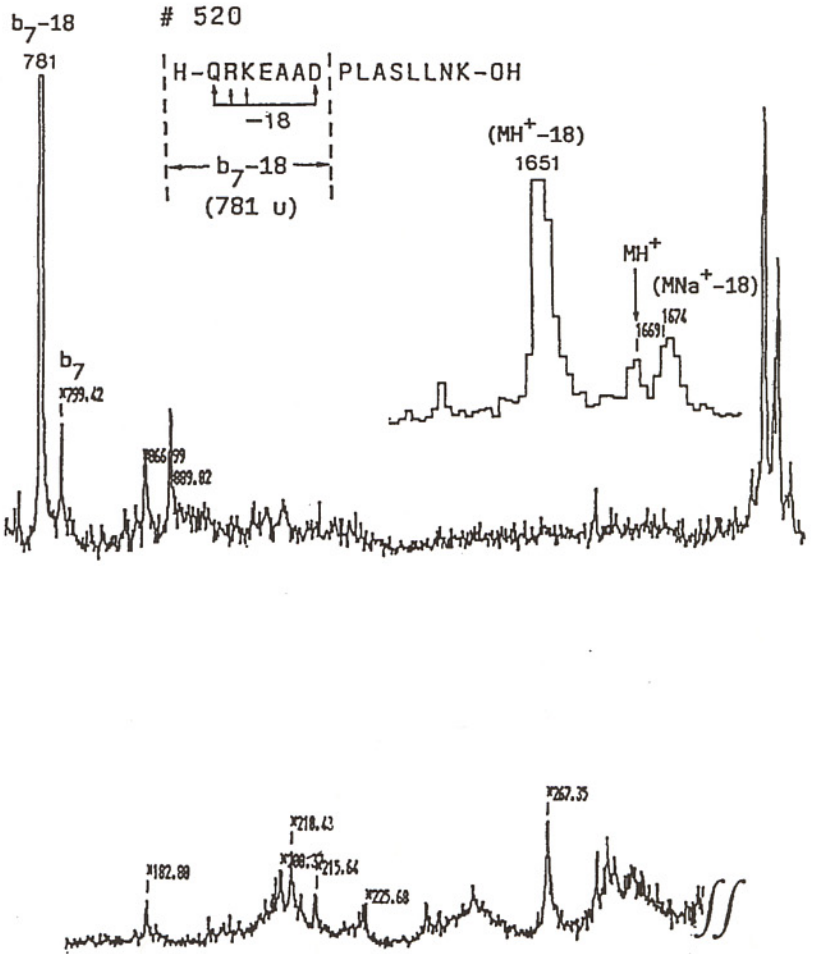

Fig. 11. PSD fragment ion spectrum of a synthetic peptide (# 520, 1668 u) internally crosslinked as indicated by the loss of 18 u (H_2O) with respect to the calculated parent mass. Possible crosslinks (supposed to involve a carboxyl and an NH_2 group) are proposed by the inset. Note that more than 90% of all fragment ions formed show up in an extremely abundant b_7-17 fragment signal which is supposed to represent the cleavage located in front of the internally stabilised part of the backbone.

Occasionally, we even saw an extraordinary predominance of that "last possible cleavage", especially if the residue forming the internal crosslink was an aspartic acid. Figure 11 shows an example of a synthetic peptide (# 520 in Table 4, 15 residues, 1668 u) for which an ESI triple quad was unsuccessfully used to try to establish its amino acid sequence. MALDI-RETOF mass spectrometric evidence suggests first of all that 90% of the parent molecules had a mass deficit of 18 u (see inset Fig. 11), indicating the loss of H_2O most probably due to internal cyclisation. The vast majority (more than 90%) of PSD fragment ions in this case appeared in the form of one single, very abundant signal at 781 u which has been identified as the b_7 fragment of the $(M-18)H^+$ precursor ending in a C-terminal aspartic acid residue. Since N-terminal fragments smaller than $n = 7$ were completely absent, except for a rather prominent signal at 129.1 u (b_1), we suppose that an internal amide was chemically formed between the asp_7 and the arg_2 residues prior to mass analysis. Similar predominances of asp-directed b- or y-type fragmentations have been observed in gamma-MSH and ACTH, both containing asp at the $n = 9$ and 29 positions respectively.

Mechanisms of activation and energy transfer

We are not yet in a position to draw a clear-cut picture of the activation, energy transfer and relaxation mechanisms ruling PSD fragmentation under our experimental conditions. Nevertheless, some preliminary evidence allows us to suggest at least a rough scenario.

Basically, in line with current concepts, our present understanding of MALDI-PSD mechanisms sees fragmentation of a polyatomic ion as the result of two distinct processes separated in time, namely: (1) activation by energy transfer; (2) dissociation after intramolecular energy redistribution. Most contemporary concepts distinguish between collisionally activated and so-called unimolecular dissociations, the latter denoting those fragmentations which occur in the absence of a collision gas and as the consequence of some "in-source" excitation. Under the present experimental conditions this dichotomy is not as clear-cut as in classical MS-MS technologies, since: (1) "in-source" activation is essentially (multi)collisional; (2) the probability for "post-source" collisions in the field free drift path certainly cannot be neglected under the actual conditions [23] but, depending on residual gas pressure and ion size, can be large or small. Thus, making no ab initio distinction between the different sources of internal energy one may, in the time domain, simply distinguish between post source and prompt dissociations, although in MALDI-TOF mass spectrometry the observation of prompt fragments is a rare exception. It will, however, be shown below that in MALDI-RETOF mass spectrometry, experimental conditions can be varied such that either in source activation or high energy post source collisions become the predominant sources for energy transfer and subsequent fragmentation.

"In source" activation

The principles of desorption and ion formation in MALDI are still poorly understood (for discussion of current concepts see ref. 34). It is clear by now that, with the actual irradiances applied, photoionization and/or photodissociation cannot play any major role. Instead, energy deposition in a superficial layer of the solid state matrix, via thermal and/or pressure pulse "sputtering" [35] leads to a jet-like ejection of matrix particles with intact analyte molecules entrained. While the plume of matrix-derived particles expands with a velocity of typically $1000–1500\,m\,s^{-1}$ over a $\cos^2\theta–\cos^3\theta$ angular distribution [36], analyte molecules are being dragged by this expanding cloud and reach about half this velocity ($\approx$ 700 to $800\,m\,s^{-1}$). Results of Beavis and Chait [37], Huth-Fehre and Becker [38], and from this laboratory [36] consistently demonstrate that analyte ions emerging unaccelerated from the plume are roughly isovelocic irrespective of their mass and have a quasi-gaussian velocity distribution extending over about one fifth

of their mean velocity (full width at half maximum). Although there is certainly some analogy between plume expansion after MALDI and the classical pulsed gas jet used to entrain and cool labile compounds, it is not clear whether the hydrodynamic model proposed by Vertes et al. [39] is correctly describing the energy transfer mechanisms especially between neutral matrix and entrained guest molecules. This applies especially to the degree of expansion cooling which, if their predictions were correct, would certainly be difficult to reconcile with the extent of PSD observed during flight.

It is, however, not unreasonable to assume that the major proportion of the activation energy acquired in source stems from ion/neutral

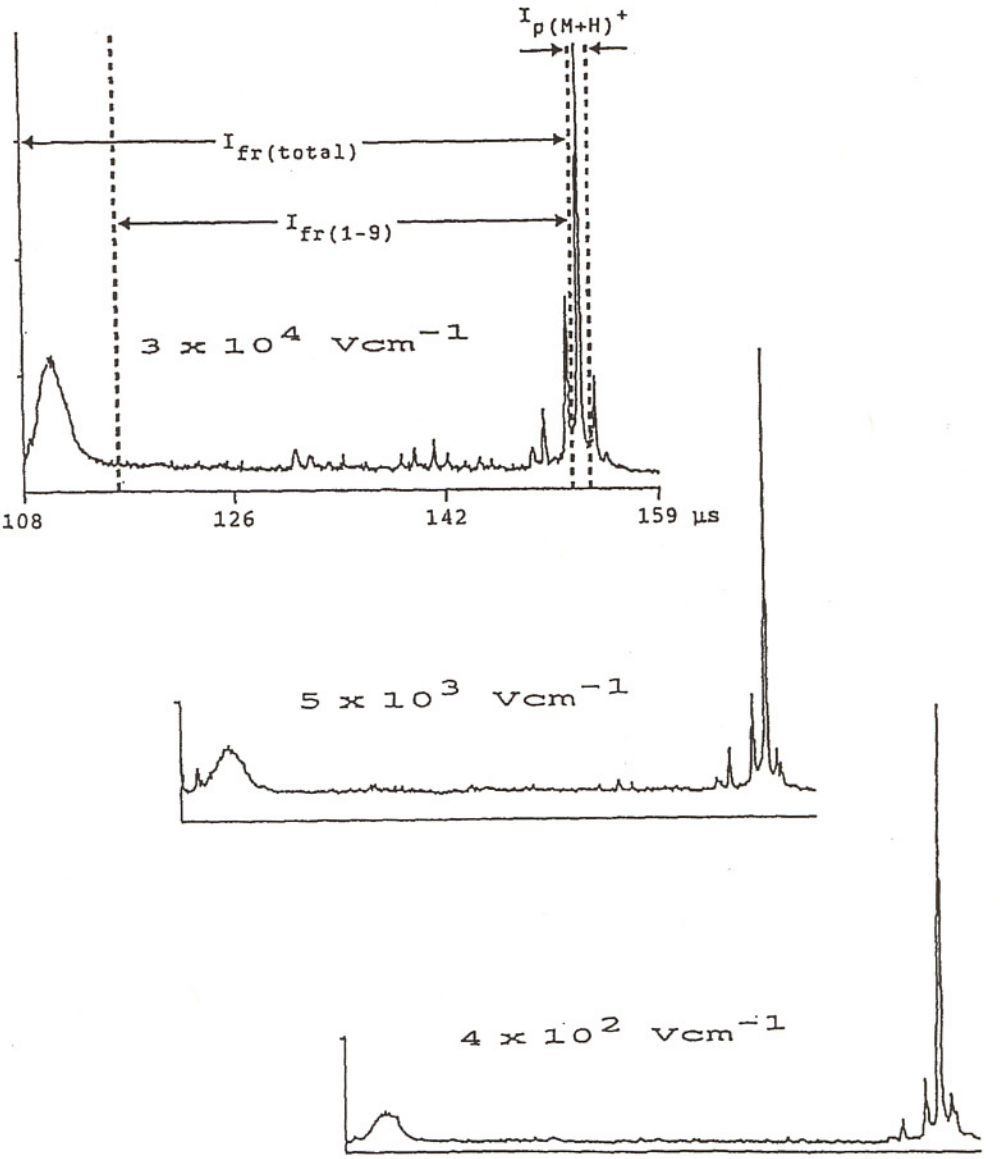

Fig. 12. Three PSD fragment ion spectra of Substance P (5 kV) with the reflectron set for parent ion recording (most of the fragment ions formed are contained in the "junk hill"). Voltage labels indicate initial field strength applied in the first distance of the split acceleration field. Note that fragment ion yield largely increases with higher extraction field strengths.

collisions under the condition that the ions rapidly gain kinetic energy from the acceleration field. Thus, one might predict that the initial electric field strength acting on analyte ions during early plume expansions, when they are still surrounded by a high number density cloud of potential collision partners (mainly neutral matrix molecules), should be a main determinant for the efficiency of PSD product formation.

By employing a split acceleration field we could experimentally confirm this prediction. As illustrated in Fig. 12, we have determined the fragment ion yield as depending on the initial field strength (E_i) in the split acceleration distance. From the data shown in Fig. 13 it is apparent

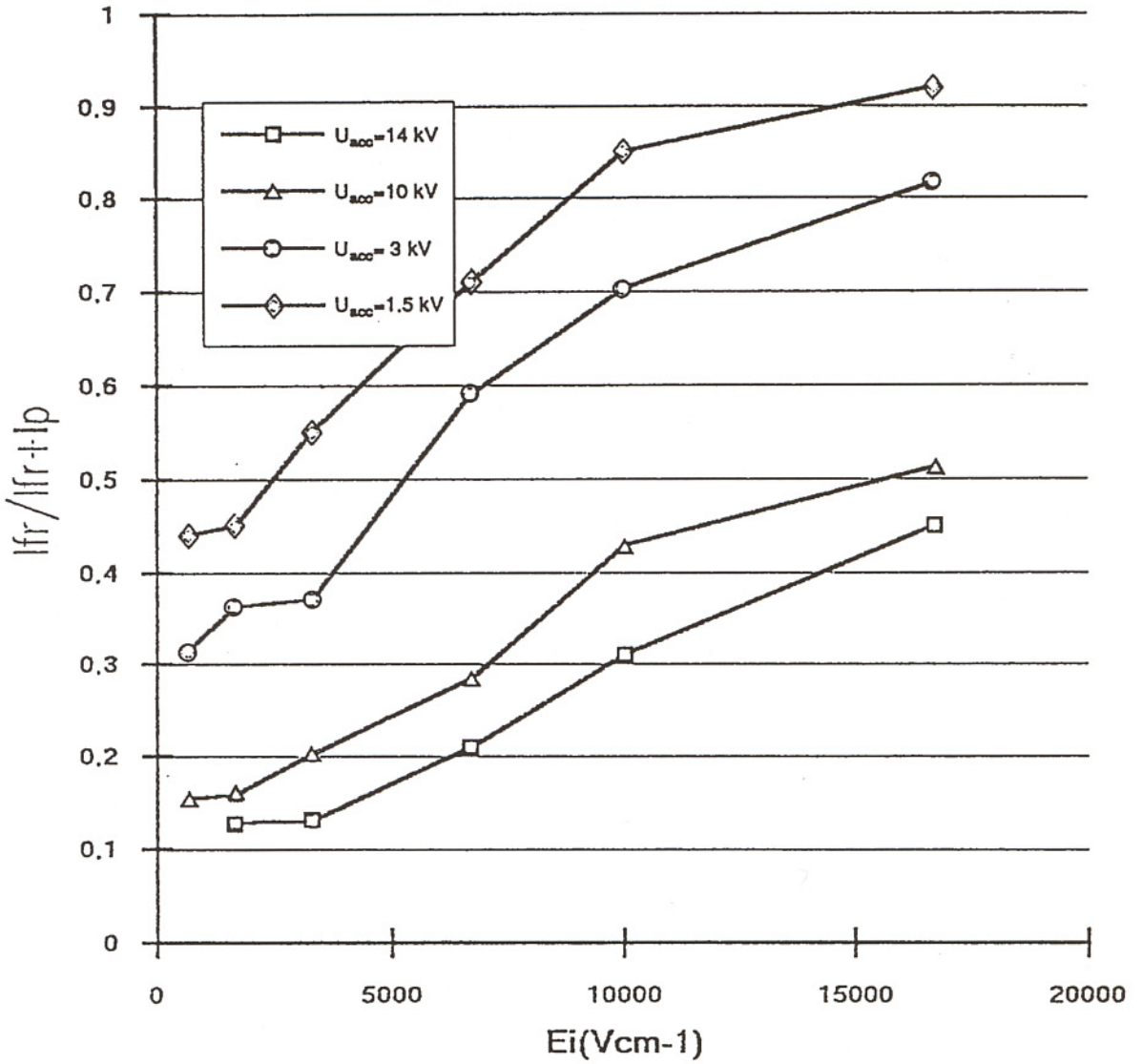

Fig. 13. Total PSD fragment ion yield (Substance P) as dependent on (1) the strength of the initial electric field and (2) the kinetic energy to which the ions are finally accelerated. I_{fr} is the intensity (peak area) of the fragment ions (the "junk hill"), and I_p is the intensity (peak area) of the precursor ion. □, $U_{acc} = 14\,kV$; △, $U_{acc} = 10\,kV$; ○, $U_{acc} = 3\,kV$; ◇, $U_{acc} = 1.5\,kV$.

that, for a given acceleration voltage (U_{acc}) of say 10 kV, the fragment ion yield of e.g. Substance P increases from 0.15 to 0.51 if E_i rises from 1.66×10^2 to 1.66×10^4 V cm^{-1}.

It is particularly noteworthy that, for a given initial field strength (E_i), the dissociation curve is shifted upwards to higher yields if the total acceleration voltage (U_{acc}) is lowered. We suspect that this is due to the prolongation of the ion flight time increasing the probability that low rate decays will occur in time. Assuming that first order kinetics rule this type of process we expect a mono-exponential decay characteristic which was found to be true after transformation of the data into the time domain (see Fig. 14).

In a given experimental situation, in source activation increases with laser irradiance in about the same way as described in one of our previous papers [25] investigating the stability of peptide ions produced by MALDI in a linear TOF arrangement.

"In flight" activation

As demonstrated in the preceeding paragraph, "in source" activation can be nearly fully prevented by choosing a very low initial field strength and irradiances close to the ion formation threshold such that the majority (more than 90%) of all parent ions formed survive the passage through the first field free drift path unfragmented. This opens the opportunity to perform "classical" CAD experiments by admitting gaseous atoms or molecules into the TOF spectrometer for high energy "in flight" collisions. To this end we simply turned off one of the two turbo pumps of our spectrometer, thereby increasing the residual gas pressure from 5×10^{-7} to $\approx 5 \times 10^{-6}$ Torr. At this pressure

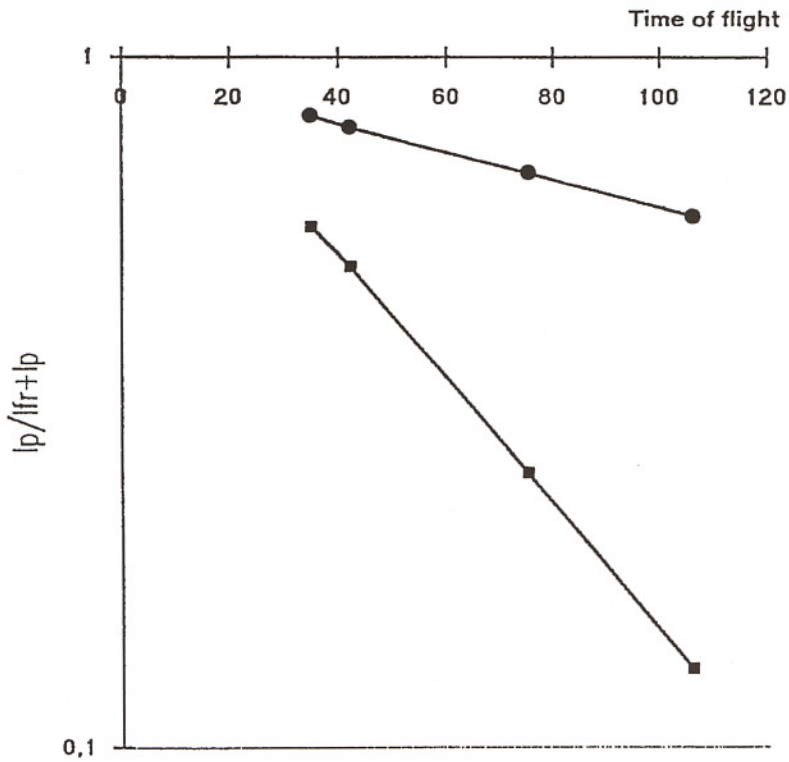

Fig. 14. Flight time versus decay rate ($(I_p/I_{fr} + I_p)$ plots) of Substance P for two different initial field strengths: ●, $E_i = 3.3$ kV cm^{-1}; ■, $E_i = 10$ kV cm^{-1}. Data were taken from the data set of Fig. 13 by calculating the flight times in the first field free drift path for the different U_{acc} values applied.

the intensity of Substance P parent ions decreased to about 30–40% of its initial value. Thus, the criterion of "optimal collision pressure" as defined by e.g. Neumann et al. [40] is fulfilled, meaning that the probability of a collisional encounter during flight is unity.

Figure 15 illustrates the experimental protocol: the experiment performed on Substance P started

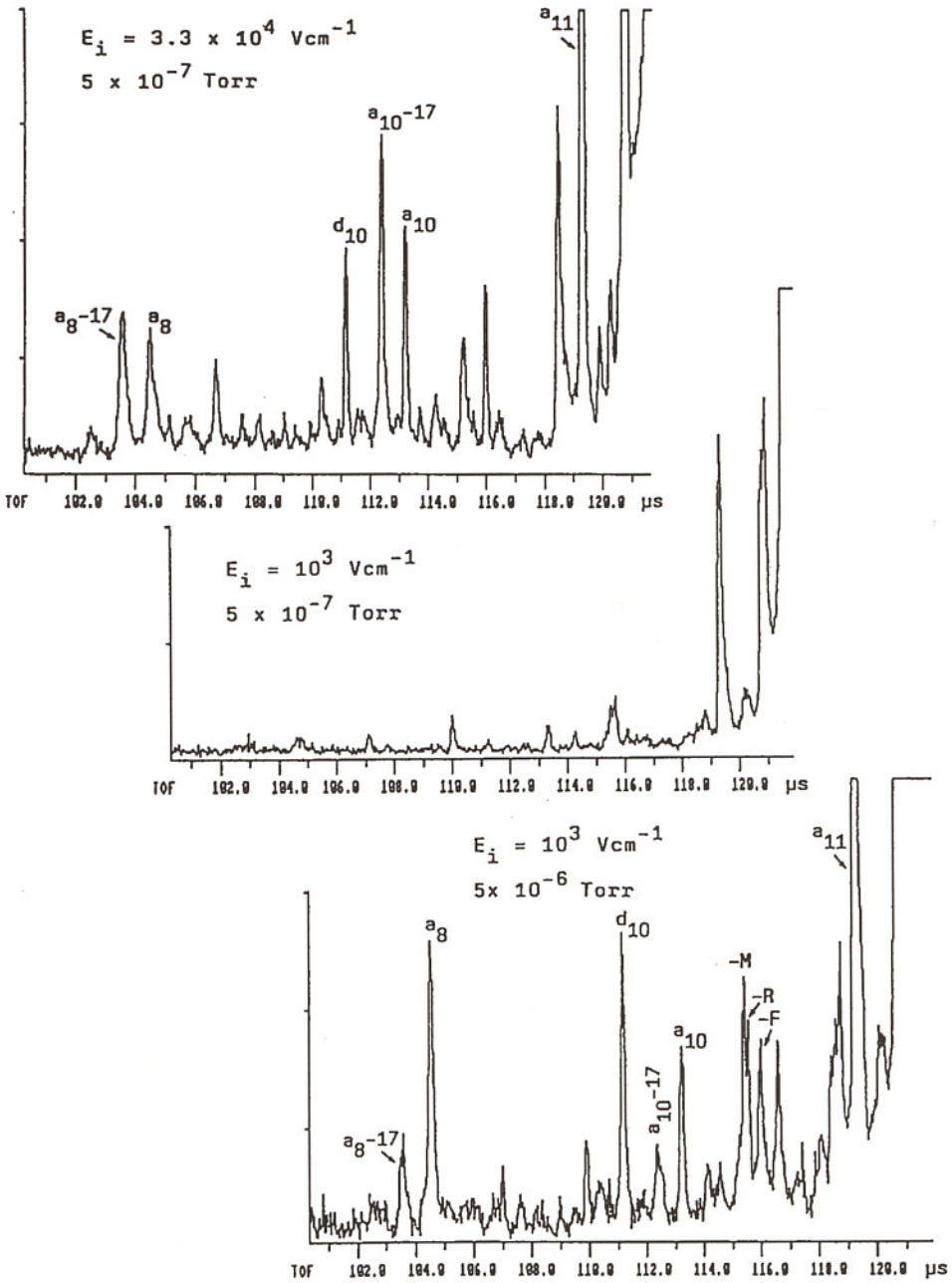

Fig. 15. Fragment ion spectra of Substance P (first segment with reflector potentials set for parent molecule recording) under different experimental conditions. See text for a further explanation.

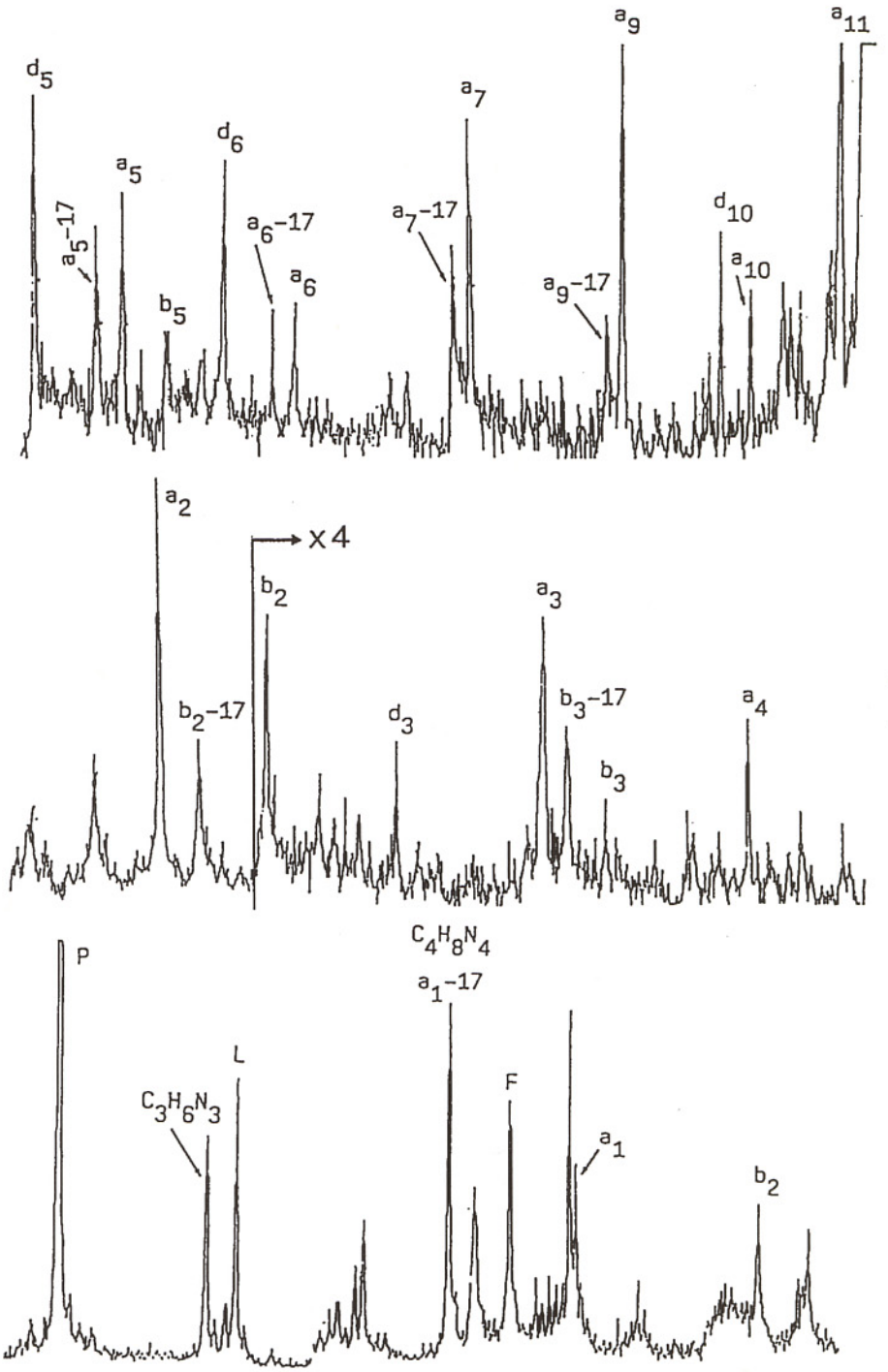

Fig. 16. CAD (residual gas) fragment ion spectrum of Substance P obtained at low extraction field strength (5×10^2 V cm^{-1}) but increased residual gas pressure (5×10^{-6} Torr) of the RE-TOF vacuum. See text for a further explanation.

with recording a usual PSD fragment ion spectrum at high initial field strength ($3.3 \times 10^4\,V\,cm^{-1}$) and low residual gas pressure (5×10^{-7} Torr). The segment spectrum shows the typical cleavage pattern characteristic for fragmentation under unimolecular PSD conditions (see above). Reducing the initial field strength to $10^3\,V\,cm^{-1}$ at the same background pressure led to a 90% suppression of the fragment ion formation. In a third step background pressure was raised to 5×10^{-6} Torr keeping the initial field strength low. Under these conditions fragmentation occurs again but with a different fragmentation pattern. While the $a_n - 17$ satellites are largely reduced, the fragment ion spectrum is now merely dominated by a_n and some d_n and b_n cleavages (see, for comparison, the full fragment

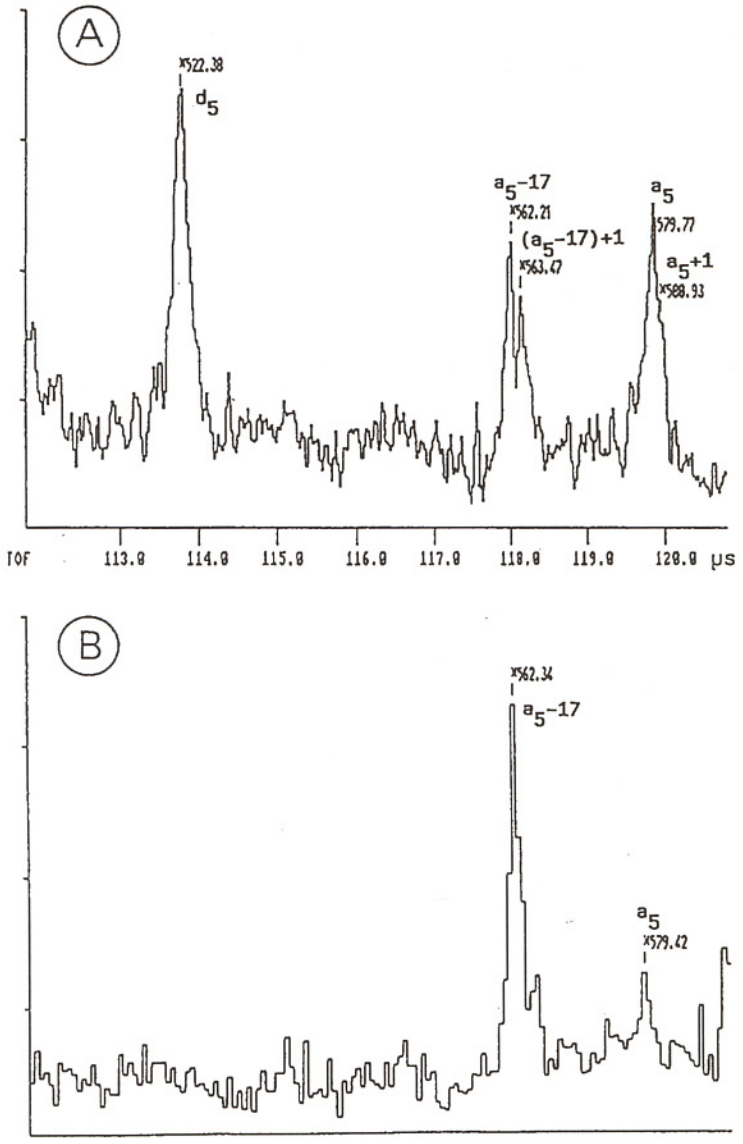

Fig. 17. Section of the fragment ion spectrum of Substance P at instrumental conditions forcing collisions with residual gas molecules ((A) postsource CAD at $U_{acc} = 10$ kV) and forcing in-source activation ((B) unimolecular PSD, high energy collisions with residual gas molecules suppressed).

ion spectra shown in Figs. 16 and 6 respectively). These fragment ion spectra very much resemble classical high energy CAD spectra of Substance P as obtained in four-sector instruments [5,29].

Particularly noteworthy is the formation of d_n fragments which, from the viewpoint of its energetic requirements, is a rather demanding process. It involves a two-step reaction of first a homolytic backbone (C-C) cleavage (free radical) followed by a side chain α-cleavage [41] and, thus, is an important indicator for a high degree of internal activation. In line with the experimental evidence given by Johnson et al. [41], in our CAD-TOF mass spectra of Substance P we nearly always saw a distonic $a_n + 1$ product ion occurring in conjunction with the appearance of d_n fragments (see Fig. 17).

Another peculiar difference between "in source" activated PSD and "post source" CAD spectra concerns small fragments (i.e. below 70 u). Not only is the relative yield of these products much larger in the latter than in the former case, but also the fragmentation patterns are distinctly different.

As shown in Fig. 18, the two fragment ion spectra share the immonium ion signals for proline (70 u), dissociated Na^+ (23 u), and the common $C_3H_6N_3$ (84 u) fragment moiety, but are otherwise rather incongruent. Particularly noteworthy in the CAD spectrum are the grouped signals at 39, 41, 43, 44 u and at 55, 56, 58, 59 u which, together with the prominent signal at 18 u (NH_4^+), would be rather indicative of partial side chain cleavages.

These findings support a model of collisional activation of macromolecules proposed recently by Uggerud and Derrick [42]. In their theory of impulsive collision the efficiency by which collisional energy (in the center of mass frame) is transferred into internal energy is determined by the ratio of the mass of the collision partner and the mass of that atom (or atom group) within the macromolecule which is actually "hit". Efficiency of energy transfer becomes maximum if these two masses are about equal. This would indeed be the case under our conditions if we assume H_2O or N_2 being the most probable collision partner and say C, O or N (with their H satellites) being the entities hit during a

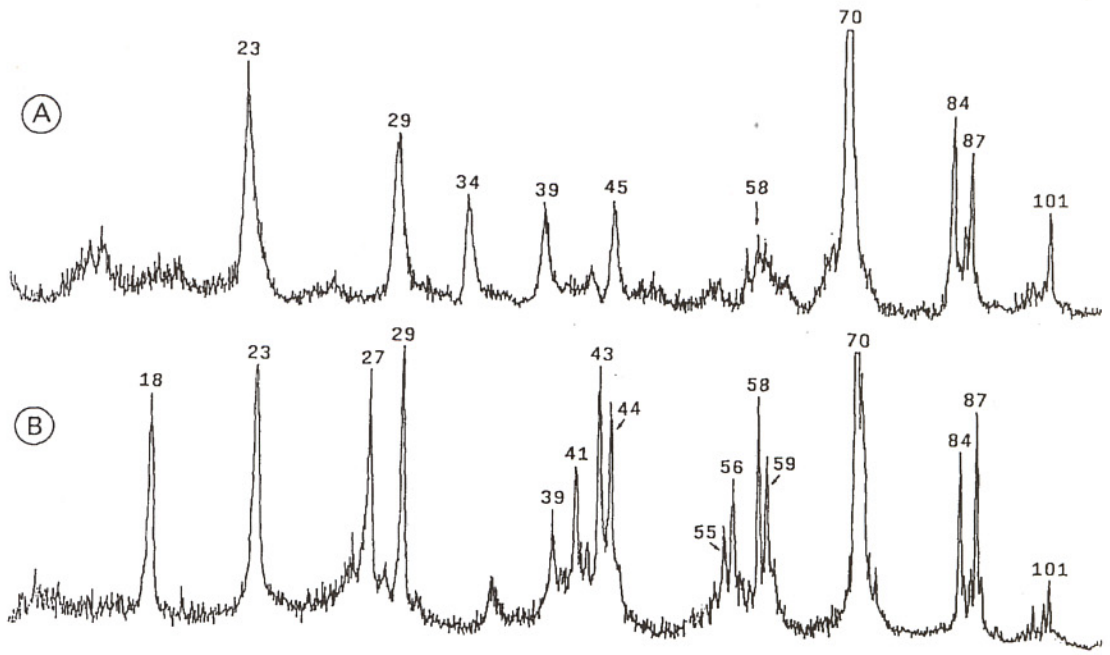

Fig. 18. Comparison of small ($m/z \leqslant 100$ u) fragment ions obtained from Substance P after either PSD (A) or CAD (B). Experimental conditions for PSD are as given in Fig. 6, for CAD as given in Fig. 16. See text for a further explanation.

collisional encounter. One of the consequences of this theory is the prediction that, with collisional energy increasing, such highly "localised" momentum transfer reactions will eventually induce immediate fragmentation at that particular location. In the case of a linear peptide this would mean that numerous small fragments should be formed by collisional "dissection" of protruding side chain groups being at much larger risk of being hit than the core of the backbone chain.

If this picture is basically true, increasing the collisional energy in the classical (high energy) CAD experiment would not be a good strategy, since it would merely augment the yield of "unspecific" fragmentations. However, the case of multiple low energy collision to sum up internal energy by relatively small increments might be much more favourable. Here, by "soft" activation, more energy can eventually be dumped into the internal energy pool without the risk of a hit-and-break event occurring. We assume that under the conditions of matrix-assisted laser desorption, and possibly also "field" excited ESI, these requirements can be met. Besides an increase of the unimolecular decay rate constants the efficiency of subsequent high energy collisional activation is probably increased by this mechanism.

What makes MALDI-RETOF mass spectrometry rather unique in the frame of approaches to fragmentation of large polyatomic ions is the conjunction of three circumstances. These are: (1) an efficient "in-source" activation; (2) the ease of providing for additional alternative high energy collisional activation during flight; (3) a large time window to accommodate even those subsequent fragmentations which occur at comparatively low rate constants.

Acknowledgements

Financial support by the Bennigsen-Foerder-Program of the Ministry of Science and Research (NRW, Germany) is gratefully acknowledged. Some of the peptides tested were provided by E. Jaeger (Max-Planck-Institute of Biochemistry, Martinsried, Germany) and M. Mann (European Molecular Biology Laboratory, Heidelberg, Germany).

References

1 F.W. McLafferty (Ed.), Tandem Mass Spectrometry, Wiley, New York, 1983.
2 G.L. Gisle and R.G. Cooks, Chem. Eng. News, 59 (1983) 40.
3 R.A. Yost and C.G. Enke, Anal. Chem. A, 51 (1979) 1251.
4 A.J. Alexander, P. Thibault, R.K. Boyd, J.M. Curtis and K.L. Rinehart, Int. J. Mass Spectrom. Ion Processes, 98 (1990) 107.
5 M.F. Bean, S.A. Carr, G.C. Thorne, M.H. Reilly and S.J. Gaskell, Anal. Chem., 63 (1991) 1473.
6 L. Poulter and L.C.E. Taylor, Int. J. Mass Spectrom. Ion Processes, 91 (1989) 183.
7 C.D. Bradley, J.M. Curtis, P.J. Derrick and B. Wright, Anal. Chem., 64 (1992) 2628.
8 R.B. Cole, S. LeMeillour and J.C. Tabet, Anal. Chem., 64 (1992) 365.
9 R.G. Cooks, T. Ast and A. Mabud, Int. J. Mass Spectrom. Ion Processes, 100 (1990) 209.
10 D.L. Bunker and F.M. Wang, J. Am. Chem. Soc., 99 (1977) 7457.
11 E.W. Schlag and R.D. Levine, Chem. Phys. Lett., 163 (1989) 523.
12 L.L. Griffin and D.J. McAdoo, Proc. 40th ASMS Conference on Mass Spectrometry and Allied Topics, May 31–June 5, 1992, Washington, DC, p. 1831.
13 J. Adams, Mass Spectrom. Rev., 9 (1990) 141.
14 C.J. Barinaga, C.G. Edmonds, H.R. Udseth and R.D. Smith, Rapid Commun. Mass Spectrom., 3 (1989) 160.
15 G.J. van Berkel, G.L. Glish and S.A. McLuckey, Anal. Chem., 62 (1990) 1284.
16 R.D. Smith, J.A. Loo, C.J. Barinaga, C.G. Edmonds and H.R. Udseth, J. Am. Soc. Mass Spectrom., 1 (1990) 53.
17 C.K. Meng, C.N. McEwen and B.S. Larsen, Rapid Commun. Mass Spectrom., 4 (1990) 151.
18 S. Della-Negra and Y. Le Beyec, Anal. Chem., 57 (1985) 2035.
19 X. Tang, W. Ens, K.G. Standing and J.B. Westmore, Anal. Chem., 60 (1988) 1791.
20 X. Tang, W. Ens, F. Mayer, K.G. Standing and J.B. Westmore, Rapid Commun. Mass Spectrom., 3 (1989) 443.
21 A. Brunelle, S. Della-Negra, J. Depauw, H. Joret and Y. Le Beyec, Rapid Commun. Mass Spectrom., 5 (1991) 40.
22 U. Boesl, H.J. Neusser and R. Weinkauf, J. Phys. Chem., 86 (1992) 4857.
U. Boesl, R. Weinkauf and E.W. Schlag, Int. J. Mass Spectrom. Ion Processes, 112 (1992) 121.
23 M. Karas and F. Hillenkamp, Anal. Chem., 60 (1988) 2299.
24 R.C. Beavis and B.T. Chait, Rapid Commun. Mass Spectrom., 3 (1989) 432.
25 B. Spengler, D. Kirsch and R. Kaufmann, J. Phys. Chem., 96 (1992) 9678.

26 B. Spengler, D. Kirsch, R. Kaufmann and E. Jaeger, Rapid Commun. Mass Spectrom., 6 (1992) 105.
B. Spengler, D. Kirsch and R. Kaufmann, Rapid Commun. Mass Spectrom., 5 (1991) 198.
27 R. Orlando, 40th ASMS Conference on Mass Spectrometry and Allied Topics, May 31–June 5, 1992, Washington, DC, p. 1935.
28 J. Bordas-Nagy, D. Despeyroux and K.R. Jennings, J. Am. Soc. Mass Spectrom., 3 (1992) 502.
29 J.A. Hill, S.A. Martin, J.E. Biller and K. Biemann, Biomed. Environ. Mass Spectrom., 17 (1988) 147.
30 G.R. Kinsel, J. Lindner, J. Grotemeyer and E.W. Schlag, Proc. 39th ASMS Conference on Mass Spectrometry and Allied Topics, May 19–24, 1991, Nashville, TN, p. 350.
31 P. Roepstorff and J. Fohlman, Biomed. Mass Spectrom., 11 (1984) 601.
R.S. Johnson, S.A. Martin and K. Biemann, Int. J. Mass Spectrom. Ion Processes, 86 (1988) 137.
32 R. Orlando and R.K. Boyd, Org. Mass Spectrom., 27 (1992) 151.
33 L.M. Teesch, R.C. Orlando and J. Adams, J. Am. Chem. Soc., 113 (1991) 3668.
34 M. Karas, U. Bahr and U. Giessmann, Mass Spectrom. Rev., 10 (1991) 335.
35 R.E. Johnson and B.U.R. Sundqvist, Rapid Commun. Mass Spectrom., 5 (1991) 574.
36 B. Spengler and V. Bökelmann, Nucl. Instrum. Methods, (1993) in press.
37 R.C. Beavis and B.T. Chait, Chem. Phys. Lett., 181 (1991) 479.
38 T. Huth-Fehre and C.H. Becker, Rapid Commun. Mass Spectrom., 5 (1991) 378.
39 A. Vertes, G. Irinyi, L. Balazs and R. Gijbels, Proc. 39th ASMS Conference on Mass Spectrometry and Allied Topics, May 19–24, 1991, Nashville, TN, p. 927.
40 G.M. Neumann, M.M. Sheil and P.J. Derrick, Z. Naturforsch., Teil A, 39 (1984) 584.
41 R.S. Johnson, S.A. Martin and K. Biemann, Int. J. Mass Spectrom. Ion Processes, 86 (1988) 137.
42 E. Uggerud and P.J. Derrick, J. Phys. Chem., 95 (1991) 1430.